Acta Geotechnica
https://doi.org/10.1007/s11440-025-02534-w

RESEARCH PAPER

Seismic site characterization of shallow bedrock sites in peninsular India using multiple geophysical methods

Ayush Kumar[1] · Anbazhagan Panjamani[1]

Received: 19 January 2024 / Accepted: 4 January 2025

Abstract
The shear wave velocity (V_s) profile of the subsurface soils and rocks is an essential parameter for site response analysis, stiffness estimation and seismic site classification. In field, V_s is measured using two types of survey method—borehole and surface methods—which often result in conflicting V_s profiles, leading to different stiffness representations of the same site. Moreover, seismic site classification often uses these V_s data and SPT N-values. The correlations of N-values and V_s are often used instead of measuring V_s in situ. The variability among different methods is still not clearly understood and needs to be explored. Minimal studies are available to show how these V_s profiles are comparable, and how seismic site classification varies with selection of survey method. In this study, both borehole-based and surface-based methods are used to determine V_s profiles at five kinds of geological settings spread over twenty-eight test locations in different geological formations. Variability between V_s profiles at the same location is studied, and site classification from different methods is compared, along with the scatter in individual V_s values from different methods. The local geology and subsurface layers influenced the variation of V_s. Two methods of site classification were used, based on average V_s & SPT N up to 30 m and average V_s and SPT N-values up to bedrock depth, as mentioned in the literature. At most locations, any change in site classification was not observed with a change in the survey method. However, the V_s and average V_s values vary significantly across different methods at a few geological formations.

Keywords Crosshole · Downhole · Geology · MASW · Shear wave velocity · Site classification · SPT

1 Introduction

The local geology significantly impacts the earthquake ground motion and cumulative destruction resulting from an earthquake. The characteristics of the subsurface soil can affect the amplitude, frequency, and duration of seismic waves as they travel to the surface and cause deformation. This influence is known as the local site effect and can lead to intense ground shaking, liquefaction, and landslides, causing further damage. To evaluate these hazard risks at any location, it is essential first to accurately determine the subsurface dynamic properties and classify the site's seismic characteristics [2, 13, 45, 46, 54, 57]. These are fundamental for understanding how the ground will respond during a seismic event.

As seismic survey methods continue to improve, more research is emerging that considers various regional factors that affect the local behaviour of the subsurface. Currently, the shear wave velocity (V_s) and penetration resistance from the standard penetration test (SPT) are essential parameters for classifying and assessing seismic site effects [1, 28, 38]. Different field techniques are used for the measurement of V_s as one- and two-dimension profiles. These can be broadly categorized into invasive (borehole) and non-invasive (surface) methods. Invasive methods including SPT, cone penetration test (CPT), crosshole seismic test and downhole seismic test provide discrete high resolution V_s measurements, typically in 1–2 m depth increments. Among these, the borehole seismic methods are considered more reliable as they are based on travel time measurements of P- or S-waves at the required depth of investigation [28, 33, 38, 39, 56]. They also provide

✉ Anbazhagan Panjamani
anbazhagan@iisc.ac.in

[1] Department of Civil Engineering, Indian Institute of Science, Bengaluru, Karnataka, India

Published online: 29 January 2025

samples for visual and lab investigation. In contrast, non-invasive or surface methods like Multichannel Analysis of Surface Waves (MASW) and Refraction Microtremor (ReMi) give more global information than localized ones [41]. They are less expensive, cause minimum soil disturbance and have gained popularity in recent decades. However, the interpretation of surface methods is cumbersome as it involves dispersion and subsequent inversion problems. Dispersion analysis has improved significantly and has become robust [24, 25]. However, the inversion problem remains highly nonlinear and is affected by non-uniqueness of solution. Thus, ambiguities related to the interpretation of V_s profile come into the picture [15, 28, 30]. Due to almost consistent resolution with increasing depth, invasive methods are commonly considered more reliable than surface methods. Their results are often benchmarked against the other geophysical methods [28, 34, 38]. However, very few studies have presented comparisons of V_s models derived from different invasive and surface wave tests at the same location in different geology formations. Studies on the influence of the method of V_s measurement in seismic site classification are also limited. So, the main objective of this study is to carry out detailed invasive and surface wave tests in the same location in different geological terrains and understand the outcome of seismic site classification.

This study uses multiple exploration methods like SPT, crosshole, downhole and MASW to determine the subsurface profile and estimate seismic site class in the same location in the different geological formations. These tests work as indicators of subsurface strength; however, these all measure the subsurface properties by different procedures. SPT is an in situ dynamic penetration test designed to determine the engineering properties of the soil from cross-correlations. The empirical strength of subsoil is measured in terms of the penetration resistance given by the number of blows (N-value) split-spoon sampler needs to penetrate the soil for 300 mm at different depths. Conversely, the V_s measurement methods work on the direct determination of stiffness by utilizing wave propagation properties of the subsurface. V_s can be measured directly considering the travel path between source and receiver as in borehole-based methods, or by dispersion and inversion analysis in surface methods. For ease of design procedures and analysis, design parameters like bearing capacity, shear modulus and V_s are correlated with the N-value for empirical determination [2, 5, 11, 43, 50, 52]. Hence, N-values are also often used to determine V_s and subsequently, the site class for seismic characterization studies.

2 Inter-variability of different V_s profiling methods

The time and budget restrictions in a project often mandate that a single method be used for V_s measurement and seismic site classification. Hence, it becomes quite tedious to estimate the uncertainty in a single parameter V_s being used to study seismic site response analysis or classification, as all these methods estimate the velocities using different algorithms. A crosshole survey is used to obtain a detailed in situ seismic wave velocity profile for site-specific investigations and material characterization [2, 6, 28, 33, 40, 51, 53]. This method provides the highest resolution data as the signals travel horizontally between the two boreholes. The V_s value obtained is for the specific depth of acquisition. In downhole survey the waves travel through all the layers between the source and the receiver, resulting in estimation of average V_s and, V_s of a specific layer by considering the refraction along the travel path [14, 26, 31, 36, 39].

MASW utilizes the dispersive nature of the Rayleigh waves. V_s is determined using an inversion procedure applied after a dispersion curve between phase velocity and frequency of Rayleigh wave acquisition is plotted [34, 48, 49, 55]. This method results in an average V_s values for different layers, whose thickness increases with depth. The resolution of MASW decreases with depth because phase velocities of surface waves sampling deeper depths are determined by materials of a greater depth range [47]. Moreover, surface waves with lower frequencies and thus longer wavelengths penetrate deeper into the ground, losing energy due to attenuation and geometrical spreading. Longer wavelengths average the properties of a larger volume of material, leading to less precise resolution of individual layers. The travel path of seismic waves is more global compared to the localized nature of the borehole-based methods.

There have been limited attempts in the literature to study the inter-variability of V_s measurement methods at the same location. The uncertainty in the V_s value due to variation in different determination methods leads to lower reliability in further studies like amplification through site classification and site response analysis. Seismic site classification is mainly carried out using V_s measured or determined from correlations. Earlier, Brown et al. [19] compared V_s profiles obtained from surface and borehole measurements at 10 sites, but only a single measurement was made for each technique. Asten et al. [8] conducted a blind comparison of ambient noise, cone penetrometer and seismic refraction data in glacial sediments near Wellington Harbour. Later, Boore and Asten [17] reported a similar study for two sites in California with constantly increasing

velocity profiles. They improved upon the traditional method of visually comparing the plots of the V_s versus depth for various models. However, all six sites were in the same geological setting and lacked strong gradients in subsoil stiffness. Later, Kim et al. [38] investigated a single site, thus limiting the study only to a specific subsoil condition of shallow bedrock at 15 m depth. Through the InterPACIFIC project, Garofalo et al. [34] studied three sites in Italy and France with different subsurface conditions (soft soil, stiff soil, or sedimentary rock) for the variability of V_s profiling methods. A comparable $V_s{}^{30}$ (30 m average V_s) estimate was obtained between invasive and non-invasive methods. It was concluded that the overall $V_s{}^{30}$ estimates are minimally affected by the observed non-uniqueness of V_s profiles since the variability in $V_s{}^{30}$ estimates was small. Similarly, in a blind test comparison at 11 strong-motion stations in Chile, an average relative difference in V_s between invasive and non-invasive methods was found to be $\sim$ 10% for soil layers and $\sim$ 30% for bedrock [45]. Recently, Darko et al. [28] carried out a blind comparison between invasive and non-invasive methods at six sites in Windsor, Ontario, and estimated the overall average relative difference to be within 18% for all sites. Comparable V_s profiles were obtained using different methods, which also agreed with the impedance and showed consistency in $V_s{}^{30}$ estimation. It can be noted here that $V_s{}^{30}$ is not an appropriate method of averaging the stiffness of the site to reflect amplification in shallow bedrock regions [3, 22, 46]. Moreover, the distance between the borehole or CPT point and surface wave test location in the previous studies was in the range of 100–300 m, which is very high to study the effect of different methods on V_s models. The spatial variability of subsurface properties can lead to erroneous interpretations [57].

With the wider application of $V_s{}^{30}$ and N^{30} classifications for seismic studies and their inclusion in regional design standards, it has become imperative that a wider range of geophysical tests be studied for site classification procedures. In this study, V_s profiles were obtained at the same test locations within proximity using MASW, cross-hole and downhole surveys, and SPT data. The V_s profiles obtained from various methods are compared and then used for site classification based on a 30 m average V_s ($V_s{}^{30}$) [18] and up to bedrock ($V_s{}^{BR}$) [3]. Seismic site classification of shallow bedrock sites is also studied using average SPT N and V_s value up to 30 m and engineering bedrock depth as per Anbazhagan et al. [3] and BSSC [20]. SPT N and V_s correlations previously established for this region were also used to obtain site classification and to assess the variability when compared to the classification obtained from N-values directly, as well as from V_s measurement in the same location in different geological formations.

3 Test locations

Peninsular India is one of the oldest land masses consisting of several types of geological deposits within a depth of 100 m, accompanied by spatial variations as well [11]. The region has also experienced many catastrophic earthquakes in the last 150 years. Hence, test sites are selected in a fair distribution of major geological features in south-eastern India. Figure 1 shows seven study locations where tests were carried out for the study, along with the major geological settings of Peninsular India. The geology of each test location is different, which was observed using borelogs from the investigation.

The test locations can be divided into five bins considering the subsurface geology. Residual soil deposits are found in Bangalore and Coimbatore. Bangalore lies in the south part of India at an elevation of 900 m in the Southern Dharwar Craton. The city is situated over subsurface layers of gneisses, granites, migmatites, red laterite soils and loamy-to-clayey soils. Coimbatore lies at the boundary of Dharwar Craton and Southern Granulite terrain and primarily consists of Charnockite rocks, gneisses, and granite in the subsurface. Alluvial deposits up to 30 m depth are also observed at a few locations. The coastal region of Chennai lies at the intersection of Eastern Ghats and Southern Granulite terrain and is comprised mostly of clay, shale, and sandstone. Sandy areas are found along the riverbanks and the coasts. Clayey regions are observed to cover most of the city. Alluvium and Fluvial deposits are found in Tuticorin, a coastal city where the subsurface is mostly sand, silt, and clay in varying degrees of admixture, underlain by the Charnockite group of rocks made up of gneisses in Southern Granulite Terrain. Mangalore, another coastal city, is characterized by hard laterite in hilly tracts and sandy soil along the seashore of Dharwad craton. Rock deposits like quartzites, shales, limestones, phyllites, granites, granodiorites, and granite gneiss were observed in Kadapa (in the widely popular Cuddapah Basin), with a few Alluvium deposits consisting of gravel, sand, silt, and clay. Bhubaneswar lies in the eastern coastal plains, along the axis of the Eastern Ghats mountains of Peninsular India. The subsurface in this region primarily consists of laterite, alluvial sediments, and sandstones. Surrounded by distributaries of the Mahanadi River, the alluvial sediments cover a major part of the city.

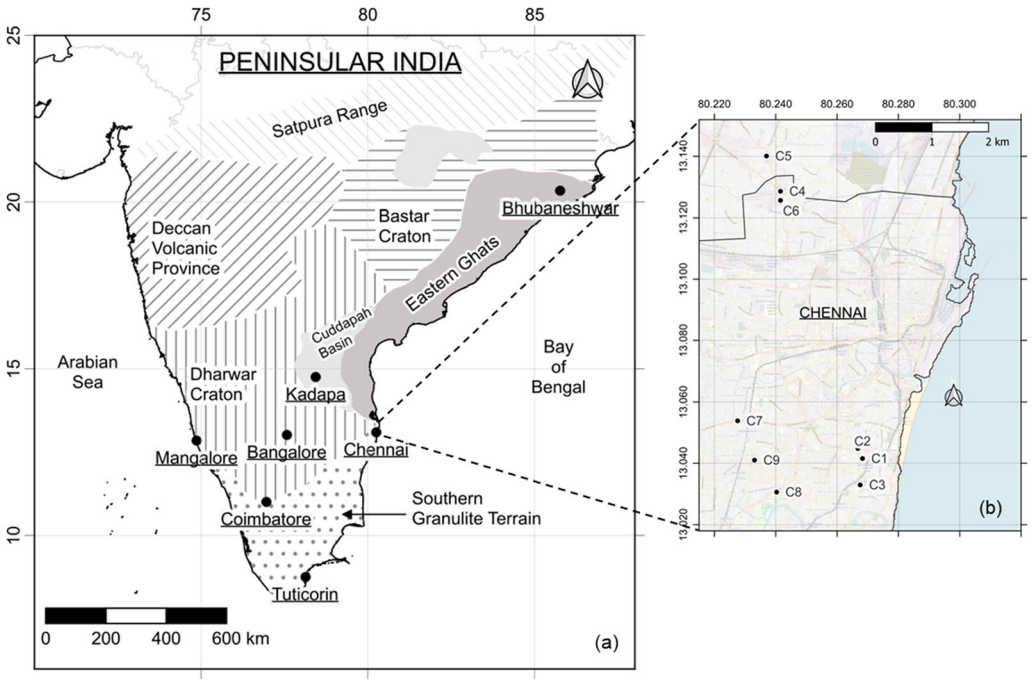

Fig. 1 Test locations in this study **a** Test locations across Peninsular India showing different geological features (after Bajaj and Anbazhagan [11]). **b** Test locations across Chennai city

4 Methodology

In this study, geotechnical and multiple geophysical tests were conducted at the test sites located across different geological terrains, as shown in Fig. 1. Boreholes were drilled at the test locations after performing the MASW survey. In a few cases, MASW was performed after borehole drilling near the borehole, as shown in Fig. 2. SPT was conducted during the drilling, and then, the boreholes were prepared for crosshole and/or downhole tests. The borehole seismic tests were then conducted, and V_S profiles were generated. The V_S profiles from different methods were then compared to understand their inter-variability with changes in the testing method. The V_S profiles were also compared with the borelog obtained previously, and the accuracy of the determination of impedance contrast was studied. In the shallow subsurface, the V_S profiles were also estimated using SPT N-V_S correlations previously developed for this region [1, 43] (in Table 1 and compared with the V_S measured from geophysical tests. These values help in studying the uncertainty incurred in the absence of geophysical tests when V_S values are obtained solely using the correlations. These V_S profiles are subsequently used to determine seismic site class based on recommendations of

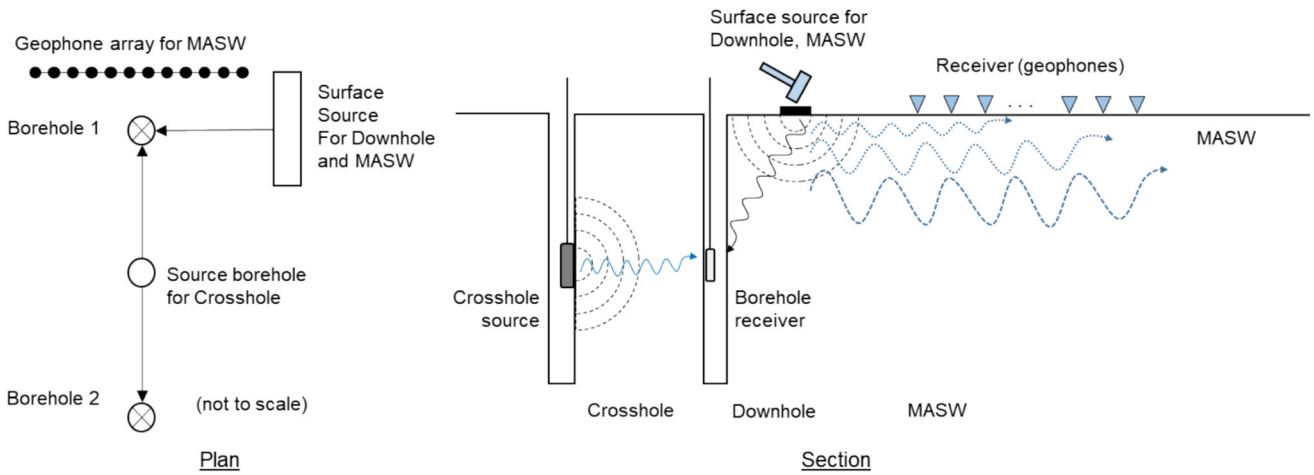

Fig. 2 Typical plan and section view of geophysical testing layout in this study

Table 1 SPT N-V_S correlations considered in this study

Correlation no	Correlation	Soils	Reference
SC1	$V_S = 95.64N^{0.301}$	All soils	[43]
SC2	$V_S = 52.21N^{0.45}$	All soils	[1]

*Both these correlations were developed for uncorrected N-values

National Earthquake Hazard Reduction Program (NEHRP) [20] based on $V_S{}^{30}$ values. Then, these $V_S{}^{30}$ values are compared with each other to study variation with changes in the V_s survey method. The presence of bedrock in shallow depth within the top 30 m was observed to affect the interpretation of site response as stiffer layers lead to high $V_S{}^{30}$ even though the soil column above may be weak [46]. Hence, apart from $V_S{}^{30}$, average V_S up to the sedimentary depth and bedrock depth is also calculated as the amplification and site response are mainly dependent upon the properties of the soil column above the bedrock.

5 Field data acquisition

SPT, crosshole, downhole and MASW tests were carried out at test locations in this study. Based on the field possibilities, the tests were carried out in a combination of two, three or all of them at the same site. SPT was performed using rotary or hydraulic drilling rigs. Crosshole and downhole tests were conducted using Seismic source BIS-SH and receiver BGK5 and BGK7 from Geotomographie GmBH. For the crosshole test, the boreholes were drilled 3–5 m apart. Crosshole tests were conducted at most locations utilizing three boreholes—one source and two receiver boreholes. In the downhole test, a 2 m long wooded beam with metal-plated ends, kept at a 2.5–3 m distance, was used as a seismic source. The MASW tests were carried out using a Geode seismograph 2 Hz or 4.5 Hz geophones using 12–24 geophones, with an 8 kg sledgehammer as an active source. Source offset was varied from quarter to half of geophone array length considering minimal near-field effects, thus avoiding contamination by body or ambient noise fields [48, 49]. The best profiles were selected based on the obtained dispersion image. All the MASW tests resulted in V_s profiles up to or beyond 30 m. The MASW survey was carried out at a distance of 1–2 m from the borehole location. The typical layout of all tests at a site is shown in Fig. 2. Each field test and typical test data are described below.

5.1 Standard penetration test (SPT)

SPT is an in situ dynamic penetration test used to determine the engineering properties of soil. It is the most widely used in situ geotechnical exploration test due to its ease of use and cost-effectiveness. The test also provides samples for testing and identification of subsurface strata. The empirical strength of the subsoil is measured in terms of the number of blows needed by the sampler to penetrate 30 cm under the impact of a 63.5 kg hammer falling from 760 mm in height. SPT N values are measured at 1 m or 1.5 m intervals up to the rebound layer. Several factors affect the N-value measurement, such as hammer energy, borehole diameter, sampler lining and overburden pressure. These factors are accounted for using correction factors. However, most of the site response and correlation studies do not consider these corrections and rather consider only the measured N-values for further computations. Hence, in this study, only uncorrected SPT N values will is to calculate N^{30} and V_S as per standard seismic site classification schemes.

N-values are later used to estimate V_S using previously established correlations for the region. The two correlations (referred as SC1 and SC2 in this study) previously developed for Peninsular India are presented in Table 1. As per NEHRP recommendations, a constant N-value of 100 is assumed after the borehole termination depth up to 30m for comparison purposes.

5.2 Multichannel analysis of surface waves (MASW)

The MASW survey is a seismic method used to evaluate the low-strain subsurface properties. This method involves a forward modelling procedure where the dispersive nature of the Rayleigh waves is utilized. The elastic properties are determined using an inversion procedure applied after a dispersion curve between phase velocity and frequency of Rayleigh wave acquisition. Rayleigh waves provide the mode with the highest energy among the various waves generated during impact and are therefore used in the analysis. Post-data acquisition, conventional signal processing techniques are used to remove ambient noise from the data and increase signal strength. Park et al. [49] and Xia et al. [55] emphasized the method's efficiency by outlining the benefits of multichannel acquisition and processing techniques well-suited for geotechnical engineering applications. Further, MASW has also been used extensively to evaluate site amplification and transfer functions for site response analysis [10, 12, 13, 23, 32, 34, 42].

This study uses a 24-channel Geode seismograph with 12 or 24 numbers of 2 or 4.5 Hz vertical geophones (based on space available) placed 1 m apart, to record surface waves generated by a sledgehammer hitting a metal plate at quarter to half array length distance from the nearest geophone. A typical multichannel surface wave record acquired from the MASW survey is shown in Fig. 3a. The multichannel waveforms are then processed using ParkSEIS software to generate a dispersion image (Fig. 3b) and extract a suitable dispersion curve with the highest signal-to-noise ratio within the desired frequency range (Fig. 3b). Then, a V_S profile is assumed and back-calculation for inversion is carried out, with further iterations till both assumed and calculated dispersion curves match with a sufficient degree of accuracy, and then the final V_S profile is obtained (Fig. 3c).

5.3 Crosshole survey

A crosshole survey is considered to be the most accurate test for the measurement of seismic velocities of subsurface layers, commonly used to obtain the most detailed in situ seismic wave velocity profile for site-specific investigations and material characterization [33, 51, 53]. This method involves the generation of seismic impulses in one borehole and recording the impulse in one or two nearby boreholes. The source and receiver are placed at the same depth. The wave velocities are determined by the horizontal distance between the source and receiver and the duration of the wave signal's travel between them (D4428-14 2014). The only demerits of the method are the high cost involved because of the drilling of multiple boreholes and the error in interpretation due to the detection of the apparent arrival of P- or S-waves [21]. The arrival time of S-waves is determined using the crossover method [36, 37], which utilizes the property of polarity reversal of S-waves when generated using impulse in two opposite directions.

The crosshole survey used one source borehole, and one or two receiver boreholes generally spaced 3 m apart at test locations. The boreholes were prepared for the source and receiver as per D4428-14 (2014), followed by borehole deviation survey to estimate the correct distance between source and receiver for survey. The source and receiver/s were then lowered at the same depth and clamped using a

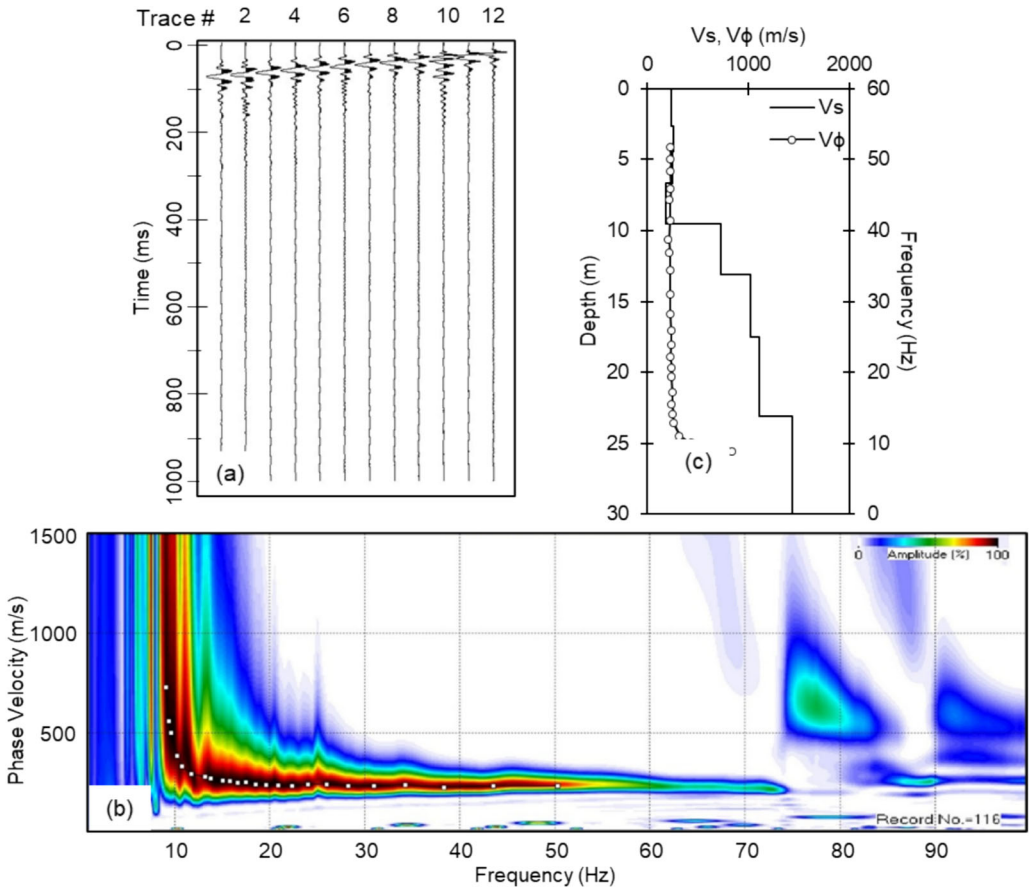

Fig. 3 MASW processing routine **a** Acquired waveform with 12 channel geophone array **b** Dispersion image with extracted dispersion curve **c** Inverted V_S profile

pneumatic packing mechanism. The source then released seismic impulses in the form of P and SH-waves (horizontally polarized shear waves) which were detected by the receiver in the other borehole. A typical schematic of wave polarization direction used for crosshole and downhole tests is presented in Fig. 4. The arrival time of the S-wave was calculated using the crossover technique [37, 44, 52], where a reversal in polarity of the S-wave with a 180° change in impulse direction is utilized (Fig. 5). The source was rotated by 180° to achieve polarity reversal, and an impulse was released again. Analysing these two opposite records together gives the arrival time. Then, from the arrival time at each depth, the V_s is obtained by considering a straight ray path from the source to the receiver.

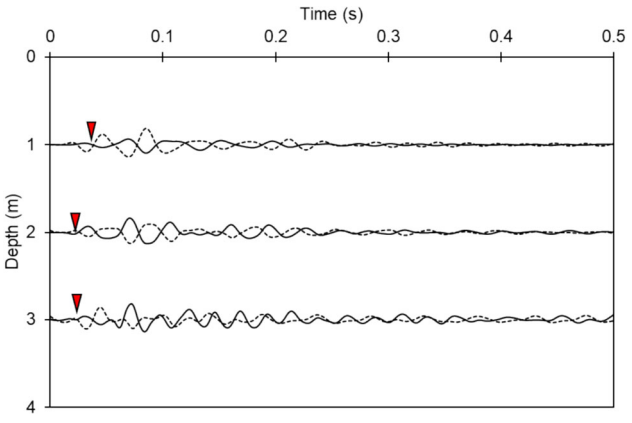

Fig. 5 Arrival time detection for typical S-wave signals in the crosshole survey using the crossover method

5.4 Downhole survey

The downhole survey is a cost-effective alternative to the crosshole survey, where a seismic source is placed on the ground surface, and the receiver is placed in a borehole. As it only requires one borehole, it is quicker and more economical. Arrival times of P- and S-waves are computed using the crossover method, similar to the crosshole test (D7400-19 2019). The velocity of subsurface layers is calculated based on the length of the travel path in different layers from the source to the acquisition depth. Since the waves travel almost vertically from source to receiver, there are fewer ambiguities about the path [26]. Most conventional methods rely on the simplified assumption of straight wave paths. However, in layered and anisotropic media, these assumptions frequently lead to inaccuracies in the velocity profile [31, 36]. Hence, Kim et al. [36] developed a method incorporating refraction due to velocity contrast along the wave travel. This method was further updated by Bang et al. [14] by integrating with the conventional direct method, to obtain V_s profiles. As per the analysis procedure, the subsurface layer boundaries are considered at the recording station depths.

An 8 kg sledgehammer and wooden shear beam 2 m long with metal-capped ends are used as a surface source for SH waves (horizontally polarized shear waves), as shown in Fig. 4, placed at a 2–3 m distance from the borehole. After hitting on one end of the beam, it was hit on the other side for a signal with reverse polarity. The crossover method, similar to the crosshole, was used for arrival time detection. Then, as discussed in Sect. 5.3, the

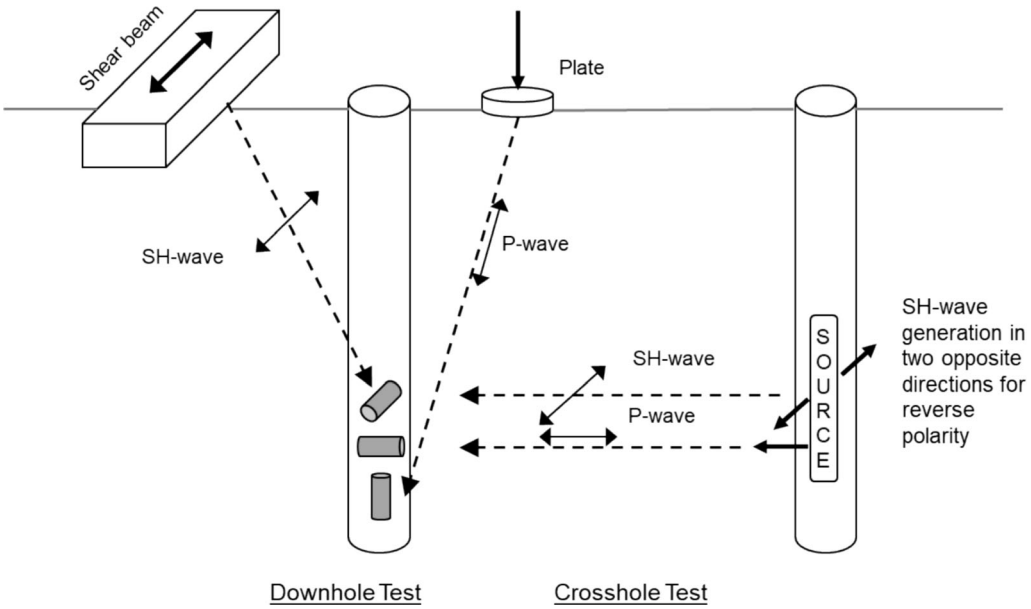

Fig. 4 Body wave types measured with crosshole and downhole tests, with a typical triaxial arrangement of geophones in the borehole receiver (after Roblee et al. [51])

V_s profile was determined using arrival times at different depths (Fig. 6). P-waves can be generated by hitting a metal plate kept at a similar distance from the borehole as the shear beam.

The test locations of the study cover the shallow bedrock region of India. In this study, the profiles are considered up to three depths, i.e. 30 m, weathered rock and engineering bedrock, irrespective of the total depth of profiles investigated. Weathered rock and engineering bedrock were considered based on borelogs and shear wave velocity defined previously [4] based on south Indian data, i.e. V_S values of weathered rock as 330 m/s ± 10% and engineering bedrock as 760 m/s ± 10%.

6 Comparison of V_S profiles obtained from different methods

The comparison of the V_S profiles obtained from the three geophysical methods is presented in this section. The borelog prepared for the test locations from SPT has also been examined to validate the accuracy of the V_S profiles. The V_S profiles obtained from the correlations are presented along with the V_S profiles determined from the field tests.

6.1 Residual deposits

There are four test sites in Bangalore's residual geology deposit (Fig. 7a and b). At location B1, one CH, DH, and MASW test were conducted. The maximum depth of the CH and DH survey was 18m. From the borelog, it was noted that the subsoil mainly consisted of silty sand up to 12 m, underlain by granitic rock. The V_S profiles from CH and DH show a gradual increase till the rock layer. However, only CH profile shows a higher impedance contrast at 11–12 m depth. The DH profile shows a more gradual

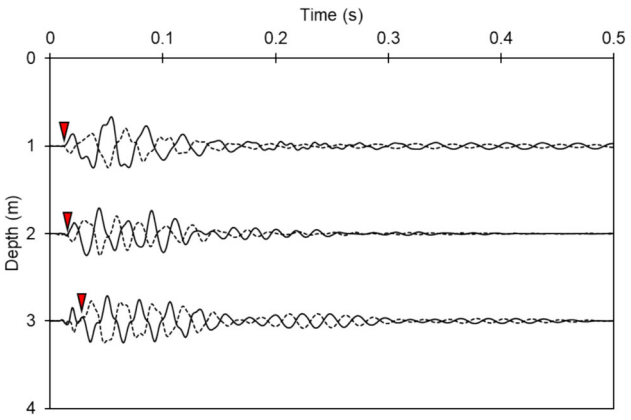

Fig. 6 Arrival time detection for Typical S-wave signals in downhole survey using the crossover method

increase in the V_S value. The MASW profiles show a constant V_S profile beyond 8 m till the survey depth and fail to capture the increase in V_S due to the soil–rock interface. The V_S profiles obtained from correlations SC1 and SC2 closely match CH and DH test results. At sites B2 and B3, CH test was not carried out because only one borehole was drilled.

At B2, the subsurface consists of silty clay, followed by silty sand and weathered gneiss rock layers, whereas at B3, silty sand is more predominant, found up to 25 m of depth, underlain by the gneiss rock system. At the B2 site, the DH profile shows a gradual increase with depth up to the bottom of the profile, with more scatter in the top layers than in the bottom. A few pockets of low velocity are observed at 2–3 m and 5–6 m. Reduction in N-values also shows weaker layer at 3 m, but beyond 4 m, N-value increases. MASW profile also follows a gradual increase in V_S with depth, showing a weak layer in a shallow depth of around 8 m, close to the soil–rock interface in the borelog. In all the profiles, silty sand layer is stiffer than the overlying silty clay layer. It is followed by weathered rock strata which has low V_s around 400 m/s.

At site B3, DH and MASW profiles agree with each other for the top 8 m. A slight reduction in N-value at 3 m is also captured in DH and MASW profiles, showing a weaker zone. The V_S values from correlations show a very gradual rise with depth, whereas in MASW and DH profiles, the V_S values show an almost constant trend up to the depth of investigation. Below 4 m, both MASW and DH show a reduction in V_S, which is not reflected in N-values.

At location B4, the subsurface comprises silty clay, sandy silt, weathered gneiss, and granite rock formations. The borehole depth limited the extent of DH and CH surveys; however, MASW profiles were obtained up to a depth of 30 m. Since the N-values show rebound at 5 m, the V_S from correlations show constant values below 5 m. CH and DH profiles agree with the V_S profile from correlations. At 2–3 m, N-values reduce showing a reduction in stiffness, whereas DH shows the presence of a weak layer at 3–4 m depth, which is also mildly reflected in CH profile. CH profile shows a significant increase in V_S values beyond 12 m, which is the occurrence of a weathered rock layer. The MASW profile identifies two V_S contrasts at 10 m and 14 m depths, the latter of which lies at the onset of the weathered rock layer. The first contrast shows a sudden increase in stiffness, which is also evident from SPT rebound at a much smaller penetration.

There were three test sites in the other residual geological deposit in Coimbatore, namely CTR1, CTR2 and CTR3 (Fig. 8), with DH and MASW surveys at all the locations. However, because of the stiff subsurface, SPT could not be conducted to any reasonable depth at CTR2 and CTR3 locations. At CTR1, sandy silt and Charnockite

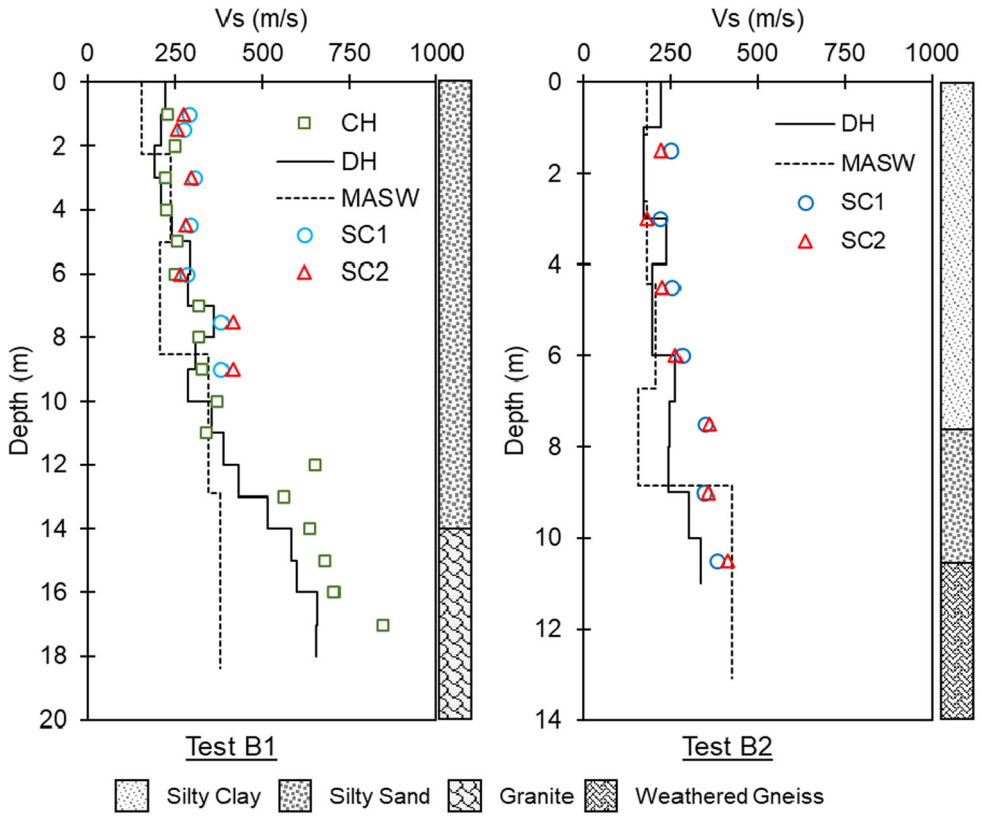
Vs (m/s)
0
250
500
750
1000
Depth (m)
CH
DH
MASW
SC1
SC2
Test B1
Test B2
Silty Clay
Silty Sand
Granite
Weathered Gneiss

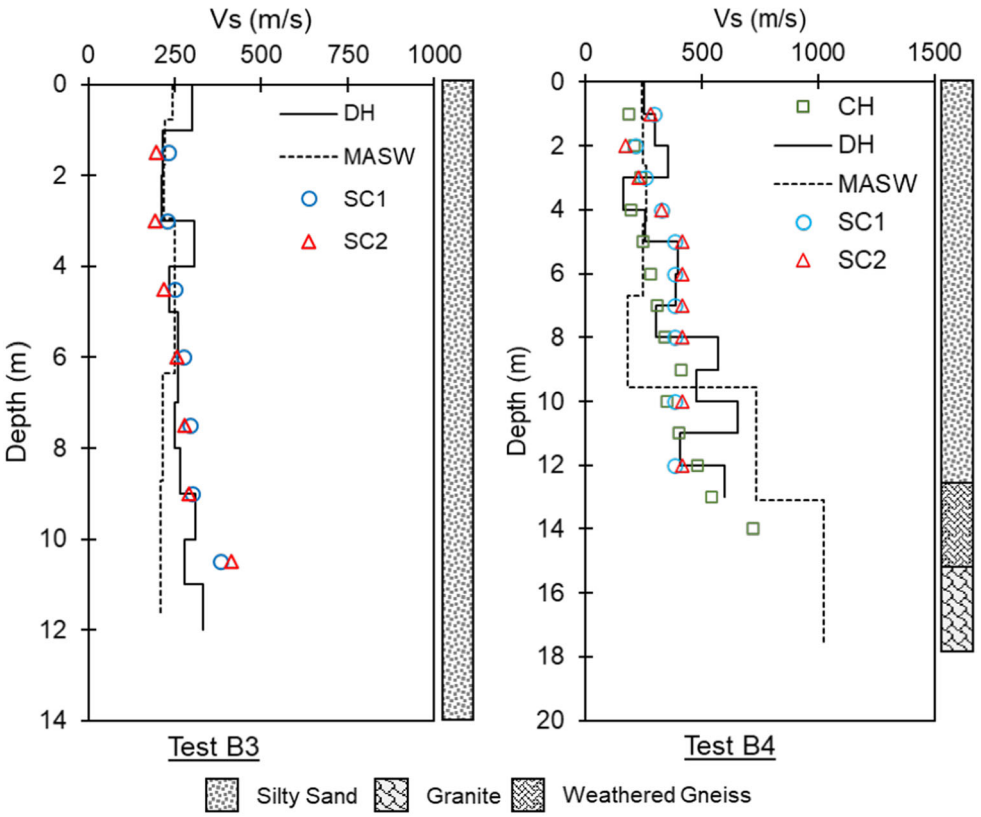
Vs (m/s)
0
250
500
750
1000
1500
Depth (m)
CH
DH
MASW
SC1
SC2
Test B3
Test B4
Silty Sand
Granite
Weathered Gneiss

◀**Fig. 7** **a** V_S profiles along with the borelog at Bangalore B1 and B2 test locations. **b** V_S profiles along with the borelog at Bangalore B3 and B4 test locations

rock formations form the subsurface profile. Both DH and MASW profiles capture a reduction in V_S in shallow depth, which is also reflected in borelog as a reduction in N-values, and hence in the V_S from correlations as well. The weathered rock zone shows a consistent increase in V_S, which matches well with the borelog, where the rock quality designation (RQD) [29] is also increasing with depth.

At CTR2, the subsurface consists of sandy silt, gneiss and Charnockite rocks. The layer of gneiss rock is highly weathered with very poor rock quality. Both DH and MASW reflect this profile as the V_S values in this layer are within the range of 500–750 m/s. At CTR3, the subsurface is formed by silty sand, limestone, gneiss, quartzite and Charnockite rocks. The limestone layer was observed to be heavily weathered with low RQD for the complete depth. Both MASW and DH profiles show the presence of a low V_S layer around 15–20 m depth, beyond which there is an increase in V_S. Towards the end of the weathered limestone layer, the V_S increases from 500 to 800 m/s to 1000 m/s followed by a further increase in the Charnockite strata.

6.2 Coastal deposits

At coastal deposits in Tuticorin, the subsurface profile consists of Silty sand underlain by weathered limestone and weathered sandstone till the investigation depth of 20 m (Fig. 9). The N-values show a gradual increase up to 9 m. In shallow depths, the V_S values obtained from CH are lower than those of DH and MASW. In soil layers, DH values are higher and predict a low-velocity layer between 1 and 5 m, which, however, is not observed in the borelog, which shows continuously increasing stiffness with depth. MASW V_S profile shows a more gradual increasing V_S profile, with V_s values lower than CH and DH after the weathered sandstone layer. The top layer of sandstone is very soft as the SPT showed rebound, but V_s values are not high.

6.3 Coastal alluvial deposits

Chennai is a coastal city, underlain by Archean rock formations as well as alluvium sediment beds. The city has nine test locations with the subsurface predominantly comprising silty sand, sandy silt, silty clay, Charnockite, and shale rock formations (Fig. 10a). At most of the locations in general, MASW V_S profiles are observed to result in higher values than the CH profiles.

At site C1, the CH profile shows an almost continuous increase in V_S values, which are also reflected in MASW profile and N-values. N-values show a rebound below

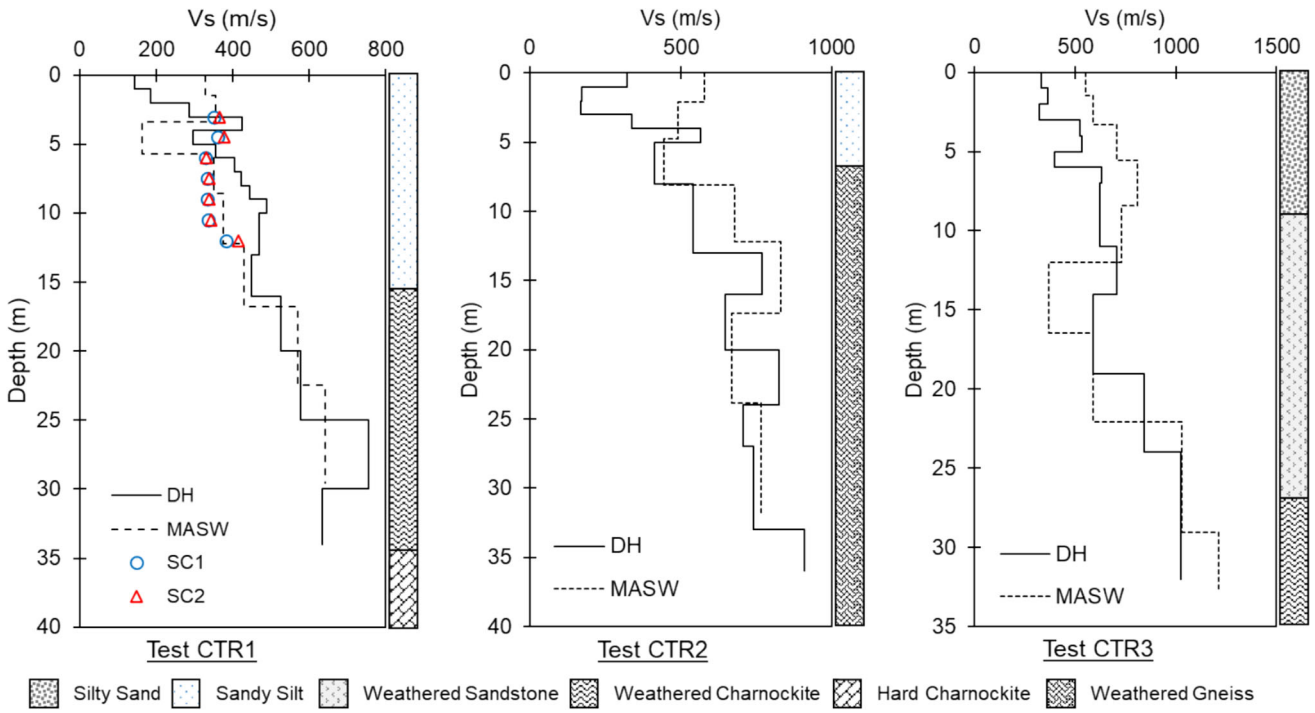

Fig. 8 V_S profiles along with the borelog at Coimbatore

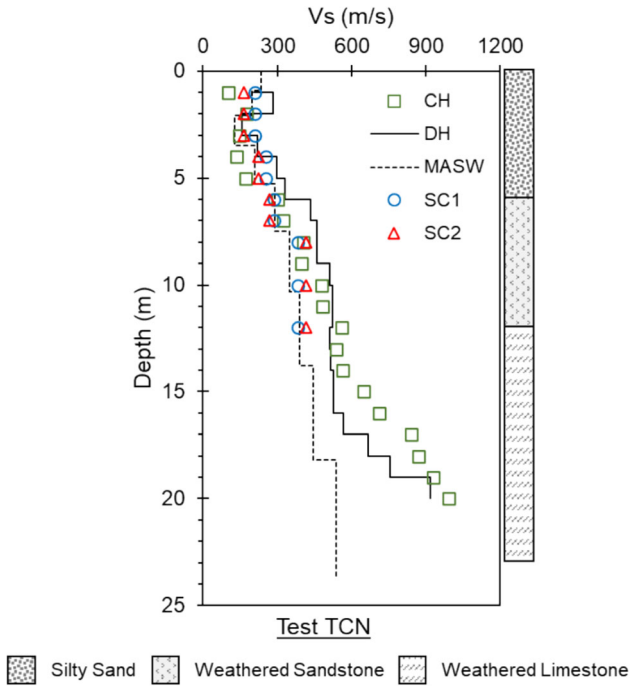

Fig. 9 V_S profiles along with the borelog at Tuticorin

18 m. However, MASW or CH profiles do not show any sharp change at that depth. The presence of weathered and hard Charnockite rock layers is also indicated in the CH and MASW profiles as a sudden rise in the V_S values. The rock quality is continuously improving with depth, as noted from borelog and evident from V_s profiles.

At site C2, both CH and MASW profiles show a constantly increasing V_S profile; however, MASW V_S values are much higher than those from CH. Subsurface heterogeneities at the test location can lead to V_s profiles which might not represent the accurate subsurface stiffness. This might be the result of more global coverage of the subsurface during wave propagation through different heterogeneous layers in larger distances [23]. MASW profile shows a very shallow interpretation of a hard rock layer at around 10 m, which is not observed either in CH profile or the borelog. The N-values continuously increase till 12 m and then decrease before rebound. However, both CH profile shows a marginal increase and MASW profile shows a sharp rise at 12 m, which does not agree with the N-value profile. CH profile increases across the weathered rock and hard rock layers with fluctuations, which agrees with the RQD values from the bedrock.

At site C3, the N-values (and V_S from correlations) and borelog show the presence of weaker soil layers below 12 m. This is also evident from CH profile, where the V_S values are low; however, the reduction is not observed in MASW profile. The V_S values show a noticeable increase at the soil–rock interface in both CH and MASW profiles; however, the CH profile shows a continuous increase in depth rather than a sudden change. The hard rock layer exhibits good RQD values, and the same is also observed in V_s profiles as well.

At C4 location, only CH profile is available, which shows an impedance contrast at the weathered rock boundary with an increasing trend further up to the hard rock stratum. Between 10 and 15 m, the V_s values are higher, but the N-values do not show any stiffer layers. At about 30 m, the RQD of weathered Charnockite strata improves and V_s also shows a jump after 30 m.

At test site C5, a good match is observed between MASW and CH profiles in shallow depth up to the soil–rock interface (Fig. 10b). Just above 15 m, at soil, there is a reduction in N-value, however, both CH and MASW profile show a sharp rise in V_S. Both profiles clearly mark the beginning of the weathered Charnockite strata at around 25 m. The rock quality is very poor and only improves towards the end of the borelog, which is also reflected in CH profile as continuous fluctuations. MASW profile shows a rather lower V_s when compared to CH throughout the rock layer.

At C6, both CH and MASW profiles show a sudden rise in V_S at the sand-weathered rock interface; however, the V_S values from MASW are much higher. The rock quality obtained from the borelog is mostly poor with slight improvement towards the end of the borehole. The RQD improves between 30 and 33 m, which is also visible in CH and MASW profiles.

At sites C7, C8 and C9, apart from CH and MASW, DH survey was also performed (Fig. 10c). At site C7, the N-value increases with depth up to the weathered shale layer. It can be observed that all the V_S profiles agree up to about 18 m depth. MASW profile predicts a sharp increment in the V_S at 18 m depth, which is not reflected in the CH and DH profiles, which show an increase in V_S after the hard rock stratum is encountered. RQD of the shale layer improves after 33 m, which is also visible in CH profile.

At C8, the V_S profile is gradually increasing for all the surveys. However, it was observed from the borelog that the N-values decreased significantly after 15 m, showing a weaker layer; this reduction was captured by CH profile, followed by an immediate increase in V_S. DH and MASW profiles show a continuous increase in the V_S values with depth in the weathered shale layer. Rock stratum is heavily fractured and does not improve till the end, only showing a gradual increase in V_s and RQD.

For C9, the MASW profile fails to detect the hard rock layer at 20 m, which is identified by the DH and CH profiles. None of the V_s profiles capture a weak layer below 5 m, where N-value decreases. Beyond this, stiffness increases with depth. In the weathered rock layer, the V_s values are inconsistent from CH, because of the fractured

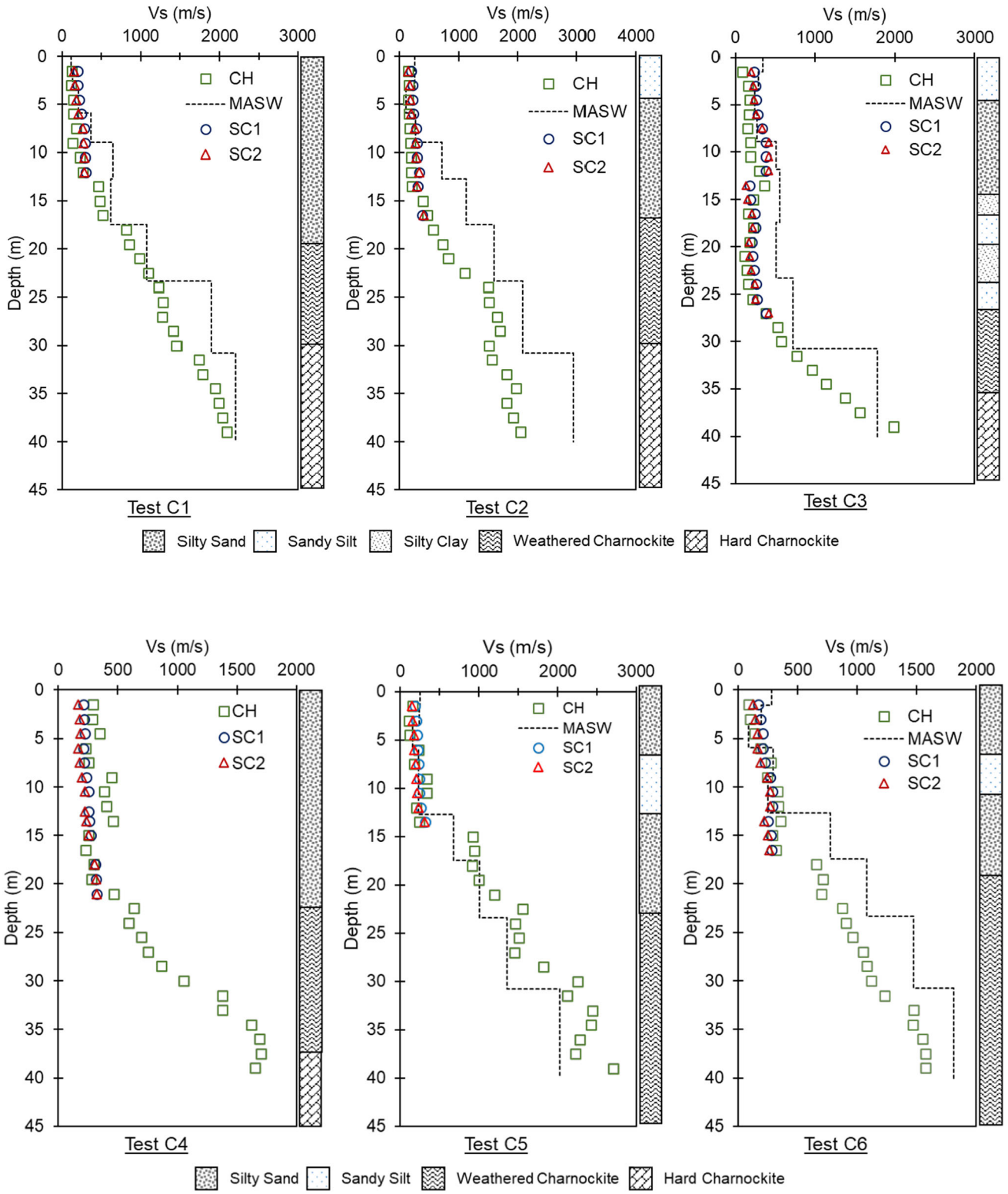

Fig. 10 **a** V_s profiles along with the borelog at Chennai C1-C3 test locations. **b** *Vs* profiles along with the borelog at Chennai C4-C6 test locations. **c** *Vs* profiles along with the borelog at Chennai C7-C9 test locations

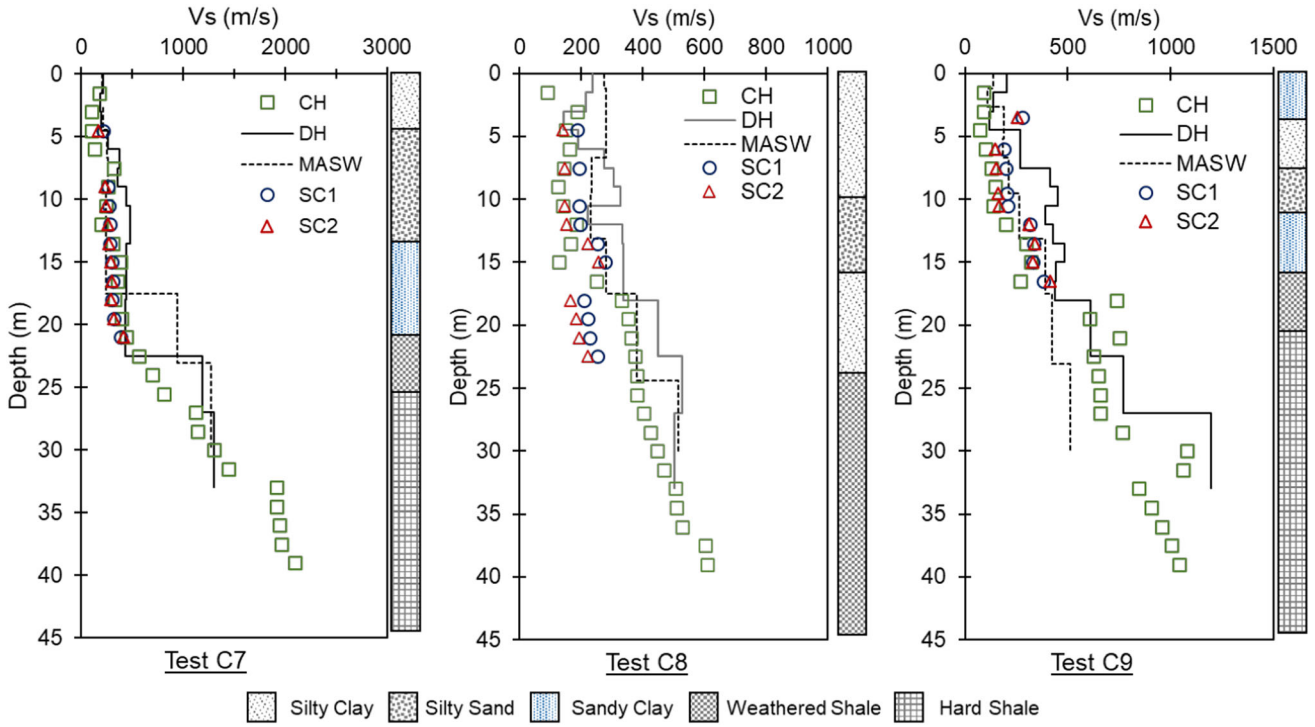

Fig. 10 continued

strata. The rock quality deteriorates again after 35 m, which is also visible in CH profile.

Alluvial deposits are also found in Bhubaneshwar, test locations BBSR1, BBSR3, BBSR4 and BBSR6 (Fig. 11a and b); these test sites are in proximity to the riverbed.

At BBSR1, DH and MASW profiles show the presence of a weak layer between 5 and 10 m, but the same is not observed in the borelog, where the N-value remains similar up to 12 m and shows weaker zones between 15 and 20 m. Another decrease in V_S is observed from DH profile after 20 m. However, MASW and N-value correlations do not show any reduction in V_S. V_S from correlations and MASW show a continuously increasing trend up to the survey depth. No rock layer is observed till the depth of investigation. However, the N-values below 25.5 m show rebound.

At BBSR3, N-values show a rebound from the first depth itself, which is also observed in DH and MASW profiles, where V_S is high in shallow depths. Beyond the recorded N-values, a reduction in V_S is observed in both DH and MASW profiles. Beyond 15 m, MASW and DH profiles show similar trends up to 30 m in weathered rock strata, beyond which DH profile shows a reduction in V_S and MASW profile shows an increase. The rock quality remains poor till the end with rock remaining heavily fractured.

At BBSR4, between 5 and 10 m, DH and MASW profiles predict a local rise in stiffness, which is not reflected in borehole data. However, at 10–11 m, both DH and MASW show a low V_s layer, the N-value from SPT also decreases there. After 20 m, all the profiles show an increase in V_S, which is the interface of soil and weathered rock, with DH profile showing a drop after 30 m. Rock quality remains poor till the end, with zero RQD.

At BBSR6, the subsurface is observed to be weak with predominantly clayey soil with silt and sand. All the V_S values up to the depth of 20 m are within the 100–200 m/s range. A lower stiffness region between 10 and 15 m is observed from SC1, SC2 (or N-value profile) and DH profiles. The borehole was terminated at 20 m without reaching rebound.

6.4 Lateritic deposits

Bhubaneshwar consists of two locations with lateritic deposits, BBSR2 and BBSR5 (Fig. 11a and b). At BBSR2, SPT indicated rebound at a very shallow depth, and the weathered rock layer prohibited any further SPT. MASW profile shows a high V_S layer under 5 m depth, which is also discovered in borelog, with high RQD values. Below this layer, the rock quality remains poor. DH profile is almost constant up to 15 m, beyond which MASW and DH profiles both indicate two major increments in V_S which reaches up to 1500 m/s at the interface between sandstone and shale rocks.

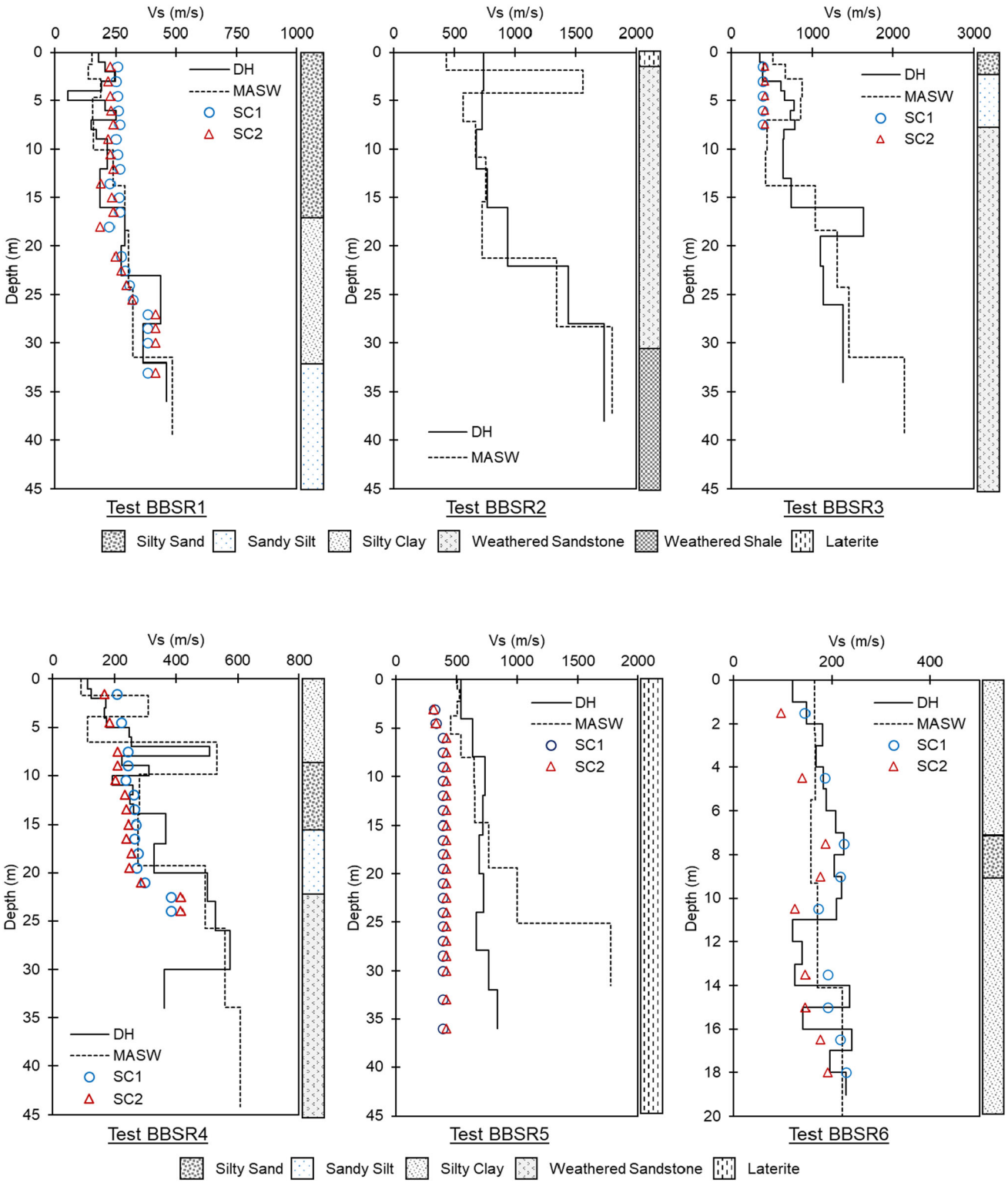

Fig. 11 **a** V_S profiles along with the borelog at BBSR1, BBSR2 and BBSR3. **b** V_S profiles along with the borelog at test locations BBSR4, BBSR5 and BBSR6

At BBSR5, cemented laterite, mostly powdered and particulate in nature, is found in the subsurface. No rock sample is obtained, and all the SPTs show rebound up to the depth of the survey. DH and MASW profiles show an almost constant V_S value up to 20 m depth. After 25 m, the MASW profile shows a significant increase in V_S; however,

the borelog does not indicate any improvement in stiffness, very similar to DH profile.

At Mangalore, the subsurface consisted of silty sand, silty clay, and lateritic deposits, underlain by granitic gneiss rock layers. V_S profiles obtained using a downhole are presented in Fig. 12. It can be observed that in the shallow subsurface, the profile generally increases with depth. In deeper depths, a few velocity inversions are observed in the granite rock layers.

At M1 location, borelog shows a reduction in N-value after 5 m, and it increases only after 14 m. A similar trend is observed in DH profile, where a low velocity zone is detected between 5 and 18 m. With the onset of Gneiss stratum, V_s increases, only to decrease again at the granitic interface. Although the rock quality remains good from 25 m onwards, the V_s is low in 25–30 m depth.

At M2, the V_S from downhole exceeds the V_S values from the correlations. A reduction in stiffness between 5 and 15 m is mildly observed in DH profile. SPT also shows higher N-values in the top 3 m and then lower N-values up to a depth of 15 m. Beyond 15 m, V_s remains constant up to the weathered gneiss layer and reduces in the granite layer, although the rock quality is very good.

6.5 Quartzite formations

The subsurface profile at Kadapa entirely consists of weathered quartzite rock formations. Silty sand layer and gravel are observed in a very shallow depth of 0.5–1.0 m (Fig. 13). The borehole depths were 15 m, and hence, the depth of CH and DH surveys was carried out up to 15 m. Because of shallow rock layers, the V_S values are high in shallow depths. The low resolution of the MASW profile compared to crosshole or downhole prevents a detailed description of V_S; instead, we get an average constant V_S value for a much higher layer thickness. Another interesting observation is the inconsistency between crosshole and downhole V_S values. It is to be noted that the subsurface consisted of moderately to highly fractured quartzite rock. The fractures and fissures in the subsurface may cause such inconsistency in the V_S values. This site is unique since the sediment thickness is very small and rock layers are very shallow, within 0–2 m from ground level.

Because of high spatial variation, the fractured rock layers make it difficult to establish any specific profile for subsurface properties. The extent of fracture will affect the degree of contact between rocks in different spatial and vertical layers. Detailed geophysical studies of these kinds

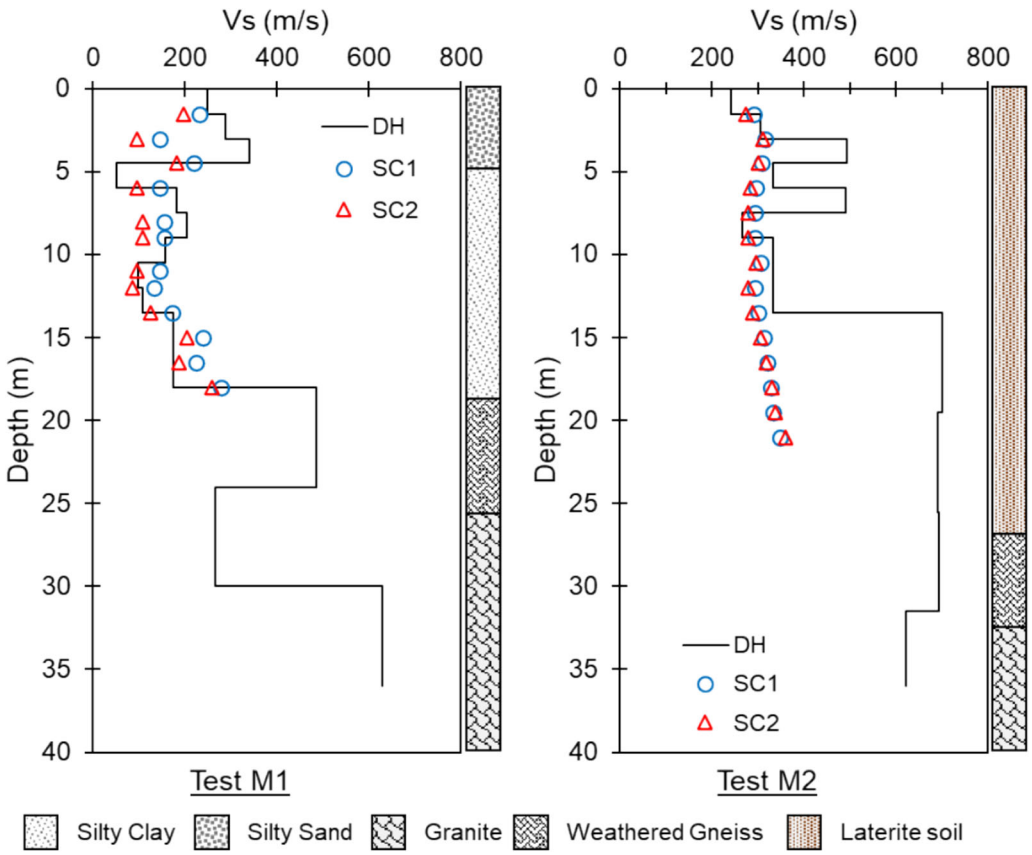

Fig. 12 V_S profiles along with the borelog at Mangalore

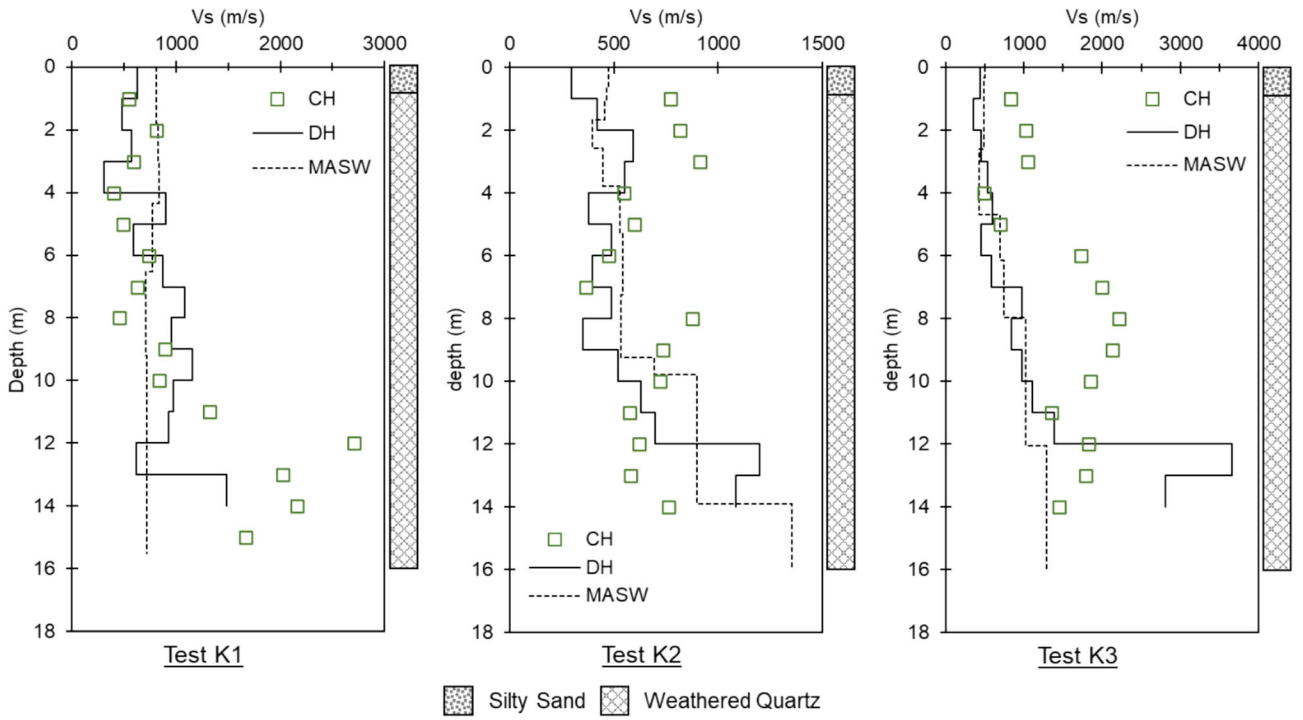

Fig. 13 V_S profiles along with the borelog at Kadapa

of sites are rare in the literature. The discussion on the influence of rock fractures on the V_S values at any depth is beyond the scope of this study.

As evident from the above discussions, variation between different V_S profiles can be the influence of either subsurface layers or, test procedures or both. In some test locations, we can observe very high differences between V_S profiles from CH, DH and MASW. As discussed in Sect. 6.3, a major cause of this high deviation is often the uncertainty associated with the interpretation of bedrock depth. The higher V_S prediction for the layer with a relatively lower V_S value will certainly result in higher errors. Moreover, downhole and MASW methods estimate V_S values by considering an average over a layer thickness, whereas for crosshole V_S is measured at any depth by horizontally travelling seismic waves. Hence, the influence of layer thickness is considered negligible in crosshole. One more observation is that the MASW method is not able to capture the variations in V_S within the shallow subsurface layers, which are fairly detected using crosshole and downhole methods.

6.6 *Comparison of individual measured V_S values*

When comparing V_S profiles derived from different methods, a reference profile is often used to compare with the other profiles. However, in this study, a reference profile does not necessarily imply the most correct representation of V_S in the subsurface [7]. Each method captures a different aspect of the properties at the site. DH and MASW tests represent the properties over a larger area and volume of the soil, whereas a CH test will interpret V_S only in a highly localized region at a depth. The variability in V_S at each test site is studied using the Coefficient of Variation (COV, given by the ratio of standard deviation to the mean), which implies the extent of variability in relation to the mean V_S. Hence, in some sense, this method employs the mean V_S profile as a reference profile, as COV for all the V_s values at a given depth is estimated.

The COV plots for test locations where MASW, SPT, CH and DH, all four tests were conducted are shown in Fig. 14. In residual deposits, it was observed that the COV values lie mostly within 30%. Mostly, MASW results do not match well with CH and DH results and lead to high COV values. At B1, almost all COV values lie within 30%. Below 12 m, the V_S profiles deviate more, and hence, the COV values start to rise. At B4 as well, the COV values mostly remain under 30%. Major rifts in V_S profiles are observed in weathered rock strata, where the MASW profile diverges significantly from DH and CH.

At the coastal location of Tuticorin, COV mostly lies under 30%. COV increases in the weathered rock layer as MASW and DH profiles underestimate the stiffness when compared to CH. In shallow depth, COV is higher because

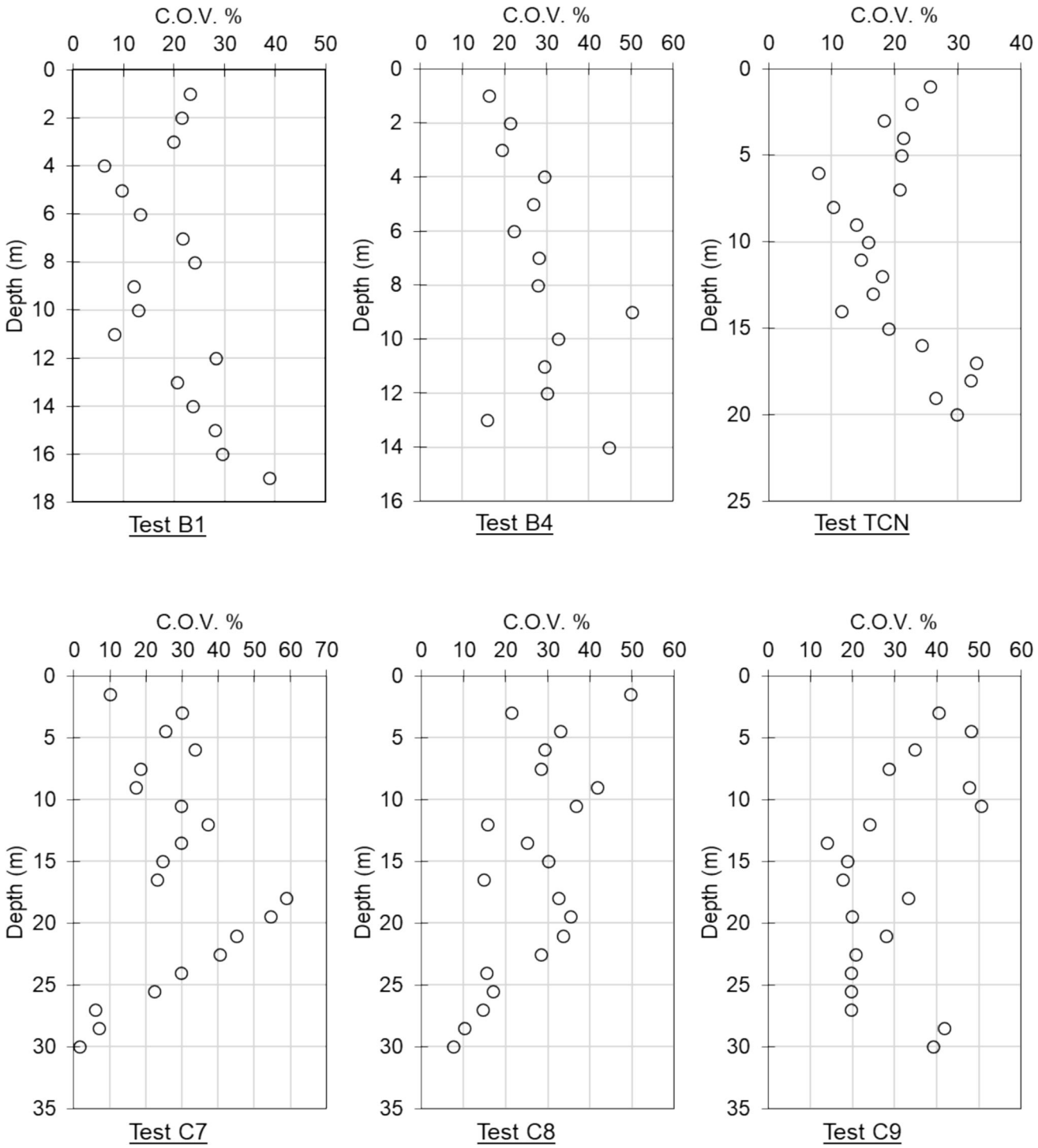

Fig. 14 C.O.V. (%) for B1, B4, TCN, C7, C8 and C9 test locations

the mean V_S value itself is low, and any small change in deviation reflects largely on COV.

Coastal Alluvial deposits show a high variability among different methods, as 43% of the data has COV > 30%. However, test locations at Bhubaneshwar show less COV when compared to Chennai. One major reason for such high COV values could be the difference in CH and MASW profiles. At C7, the underestimation of hard rock depth in the MASW profile causes high variability. At C8, DH and MASW both are high when compared to CH and correlations profile, DH predicts a high stiffness layer between 15 and 20 m, and MASW results in a constant V_S

layer up to 5 m, which leads to high COV in these depth ranges. At C9, DH results in a high V_S layer around 10 m depth, which leads to a high COV value. At quartzite locations, CH profile has much higher values than DH and MASW profiles. Still, COV remains mostly under 40%. This section only discussed COV for test locations where all four tests were conducted.

Further, the inter-variability of V_S values from crosshole, downhole and MASW were studied by comparing them with each other for the same depth and location. Figure 15 shows the 1:1 comparison of V_S values obtained from MASW, CH and DH tests. At most of the locations, relation between the V_S values obtained from the three methods does not follow any trend; however, at a few locations, clear trendlines are observed. Moreover, the number of data points is less where any relation is found. In residual deposits, V_S values from the borehole methods compared well to each other. However, both these methods had excessive scatter when plotted against MASW.

At the coastal location in Tuticorin, the relationship between the different V_S values was clearly observed, with MASW being lower than CH as well as DH, while CH and DH result in comparable V_S values. At coastal alluvial sites, DH results in marginally higher V_s values than CH, and almost like MASW. V_s values from MASW are much higher than those from CH as already seen above due to incorrect estimation of V_s contrast at bedrock depth. In general, CH and MASW results do not match well for almost all datasets, except for a few values up to 500 m/s in coastal locations. For quartzite rock formations, CH profiles have higher V_s values then DH and MASW, in general. V_s from DH and MASW are comparable at most locations, possibly because both methods compute an average V_S for a subsurface layer thickness, whereas the crosshole test gives V_S at any depth, like a point measurement. At lateritic deposits, the number of data points is less; however, except for a few outliers, the V_s results from DH and MASW compare well. So, we can conclude that MASW and DH methods can be used when average velocities of location or site are required and both cannot be replacement for CH results as it represents V_S from a particular layer.

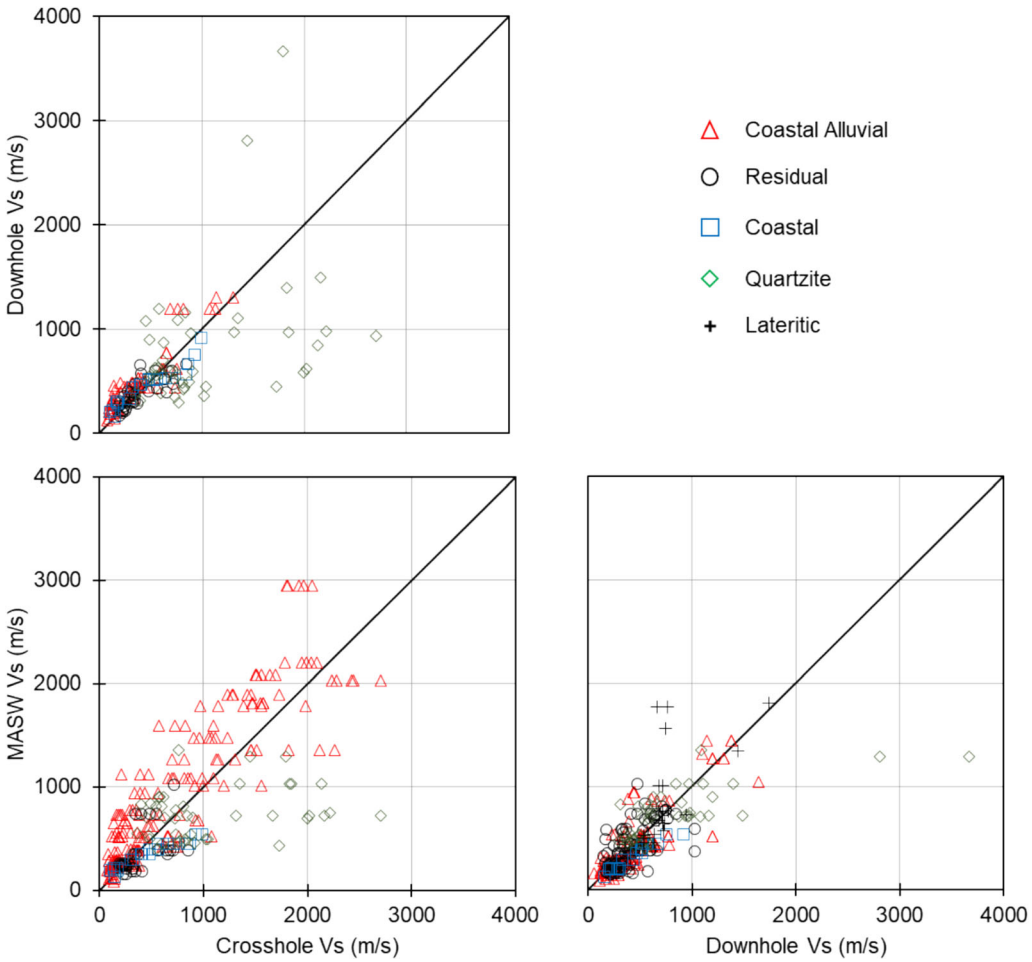

Fig. 15 Comparison of V_S values from crosshole, downhole and MASW test

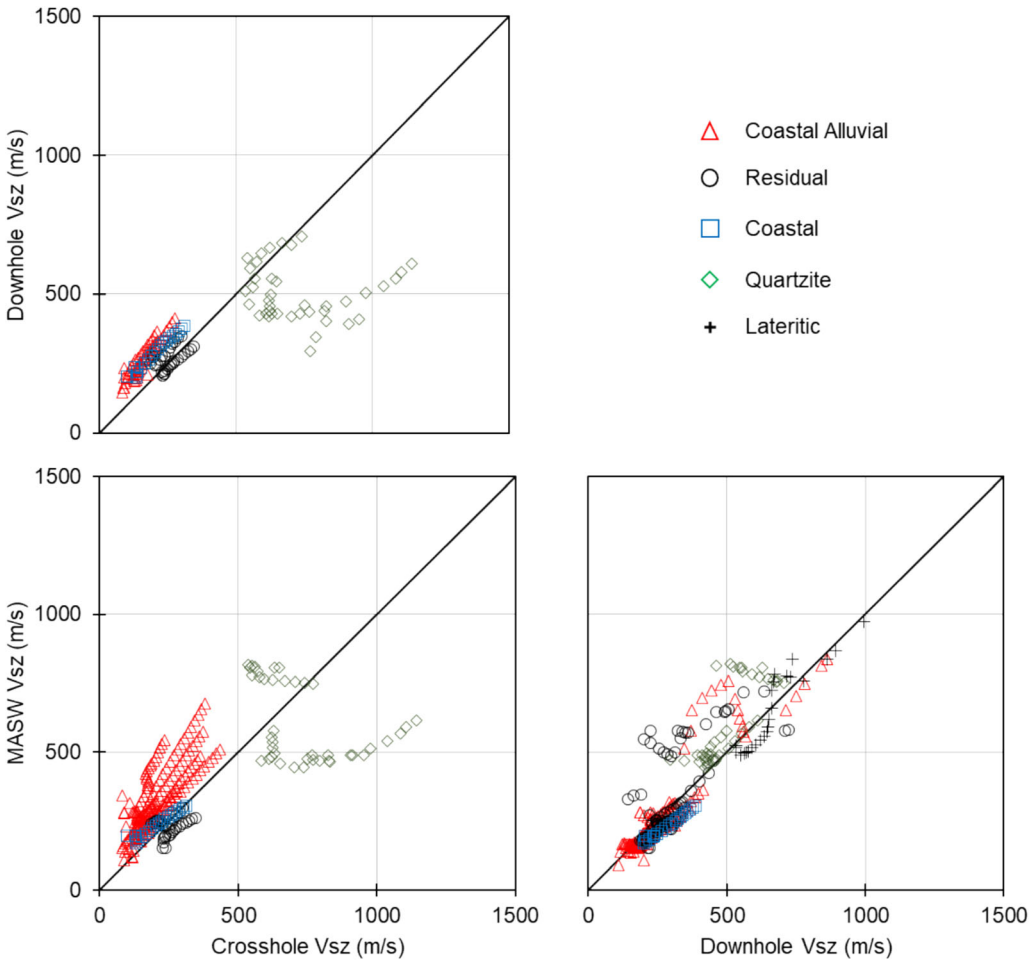

Fig. 16 Comparison of average V_S values ($V_S{}^z$) from crosshole, downhole and MASW tests

Upon further inspection, average velocities up to any depth z ($V_S{}^z$) showed less scatter than V_S. Figure 16 shows the 1:1 comparison of $V_S{}^z$ values, which shows that even though there is scatter in comparison of V_S values, different linear or curvilinear trendlines can be observed for $V_S{}^z$ for each test location, with much reduced scatter. Overall, all the plots show an increasing trend except at a few $V_S{}^z$ values. At residual test locations, the trends between the three $V_S{}^z$ values are observed to be increasing with a few exceptions. At the coastal site, there is a clear approximate linear relation between the three $V_S{}^z$ values. At coastal alluvial sites also, several linear increasing trends can be visualized from the plots in Fig. 22c, except in DH-MASW plot, where a few $V_S{}^z$ points from MASW show a reduction with an increase in DH data. At quartzite locations in Kadapa, the comparison of CH with DH and MASW $V_S{}^z$

Table 2 Site classification based on $V_s{}^{30}$ and N^{30} [20]

Site class	General description	$V_s{}^{30}$(m/s)	N^{30}
A	Hard rock	$V_s{}^{30} > 1500$	
B	Rock	$760 < V_s{}^{30} < 1500$	
C	Very dense soil and soft rock	$360 < V_s{}^{30} < 760$	$N^{30} > 50$
D	Stiff soil $50kPa \leq S_u \leq 100kPa$	$180 < V_s{}^{30} < 360$	$15 < N^{30} < 50$
E	Soil or any profile with more than 3 m of soft clay defined as soil with $PI > 20, w > 40\% \wedge S_u < 25kPa$	$V_s{}^{30} < 180$	$N^{30} < 15$
F	Soils requiring site-specific evaluations		

N: N-value from SPT, S_u: undrained shear strength, w: water content, PI: Plasticity Index

Table 3 Coefficients for estimation of $log(V_S{}^{30})$ from $log(V_S{}^{z})$, using $log(V_S{}^{30}) = a + blog(V_S{}^{z})$

Depth (z, m)	Intercept (a)	Slope (b)
5	1.994	0.735
10	1.489	0.806
15	1.129	0.854
20	0.706	0.912
25	0.335	0.959
29	0.062	0.993

showed higher values in CH, and the lowest in DH. A section of DH-MASW plot in Fig. 22d shows reduction in MASW $V_S{}^{z}$ with increase in DH $V_S{}^{z}$. For lateritic test locations, both MASW and DH tests resulted in similar $V_S{}^{z}$ values, as the points are almost colinear with 1:1 line. As a general observation from all the plots in Fig. 22, in lower $V_S{}^{z}$ range (< 500 m/s), the relations observed between $V_S{}^{z}$ from two methods are linear. Thus, these relations can be more clearly established in soil layers, in shallow depth, and the rock layers pose more challenges with more variation in $V_S{}^{z}$ values.

6.7 *Average V_S values for seismic site classification*

Site classification methods involve using shear wave velocity from measured values or obtained from SPT N-value through a correlation to indicate seismic site amplification. There are various methods for classifying the amplification potential of a region using V_s [46]. One such method is to calculate the average shear wave velocity of the top 30 m, known as $V_s{}^{30}$ is

Table 4 $V_S{}^{30}$, N^{30} and seismic site class for test locations

Location	CH		DH		MASW		SC1		SC2		SPT	
	$V_S{}^{30}$	Class	$V_S{}^{30}$	Class	$V_S{}^{30}$	Class	$V_S{}^{30}$	Class	$V_S{}^{30}$	Class	N^{30}	Class
B1	426.5	C	392.1	C	334.4	D	449.4	C	442.0	C	74.0	C
B2	NT	–	344.3	D	364.4	C	399.4	C	369.3	C	59.6	C
B3	NT	–	382.3	C	360.8	C	379.8	C	342.8	D	54.7	C
B4	418.3	C	440.7	C	487.7	C	463.1	C	461.2	C	72.9	C
CTR1	NT	–	434.4	C	405.2	C	481.2	C	491.5	C	86.5	C
CTR2	NT	–	496.5	C	645.5	C	NT	–	NT	–	NT	–
CTR3	NT	–	708.5	C	645.4	C	572.7	C	608.7	C	100.0	C
TCN	386.6	C	434.8	C	366.3	C	403.5	C	377.2	C	51.4	C
C1	299.7	D	NT	–	425.5	C	337.1	D	309.8	D	39.9	D
C2	305.9	D	NT	–	470.9	C	355.1	D	323.0	D	39.5	D
C3	188.5	D	NT	–	437.3	C	277.7	D	244.9	D	25.1	D
C4	340.2	D	NT	–		–	307.3	D	271.5	D	29.8	D
C5	349.4	D	NT	–	393.9	C	329.8	D	284.8	D	32.3	D
C6	297.0	D	NT	–	354.0	D	312.5	D	268.3	D	27.5	D
C7	277.7	D	409.7	C	349.4	D	326.9	D	297.6	D	36.1	D
C8	202.7	D	312.5	D	311.4	D	244.7	D	197.6	D	15.9	D
C9	208.9	D	366.6	C	276.9	D	332.1	D	291.3	D	31.3	D
BBSR1	NT	–	220.6	D	185.2	D	276.6	D	253.5	D	31.7	D
BBSR2	NT	–	891.4	B	819.2	B		–	NT	–	NT	–
BBSR3	NT	–	843.1	B	784.1	B	553.4	C	589.7	C	100.0	C
BBSR4	NT	–	285.2	D	270.7	D	296.1	D	264.4	D	29.9	D
BBSR5	NT	–	667.8	C	732.0	C	377.8	C	402.6	C	89.0	C
BBSR6	NT	–	229.3	D	203.0	D	259.3	D	205.7	D	NT	–
M1	NT	–	189.1	D	NT	–	238.8	D	179.9	E	10.4	E
M2	NT	–	464.3	C	NT	–	368.1	C	358.3	D	56.5	C
K1	898.4	B	843.0	B	976.7	B	NT	–	NT	–	NT	–
K2	764.9	B	629.0	C	883.6	B	NT	–	NT	–	NT	–
K3	1311.3	B	826.8	B	1012.4	B	NT	–	NT	–	NT	–

* $V_S{}^{30}$ values are in m/s, NT: No test conducted

Table 5 Soil Thickness and Bedrock Depth at the test locations

Location	Sediment thickness (m)	Bedrock depth (m)	Soil type/s	Rock type
B1	12	19	sand, silt	granite
B2	10.5	NF	clay, silty sand	gneiss
B3	20	25	silty sand	dolomite
B4	12	16	sandy silt	granite
CTR1	11.3	28.5	sandy silt	charnockite
CTR2	1.8	NF	sandy silt	granitic gneiss
CTR3	7.5	NF	silty sand	charnockite
TCN	12	30	silty sand	sandstone
C1	19.5	30	silty sand	charnockite
C2	16.5	30	silty sand	charnockite
C3	27	34.5	silty sand, sandy silt, sandy clay	charnockite
C4	22.5	37.5	silty sand	charnockite
C5	22.5	39	silty sand, sandy silt, sandy clay	charnockite
C6	19.5	39	silty sand, clayey sand	charnockite
C7	21	33	silty sand, sandy silt, sandy clay	shale
C8	24	39	clayey silt, silty sand	shale
C9	16.5	21	silty sand, sandy silt, silty clay	shale
BBSR1	NF	NF	silt, clay, sand	sandstone
BBSR2	1.7	NF	silty sand	sandstone, shale
BBSR3	6.9	NF	silty sand	sandstone
BBSR4	22.5	NF	silty clay, silty sand	sandstone
BBSR5	22.5	NF	laterite cemented sand	laterite
BBSR6	NF	NF	silty clay, silty sand	
M1	19.5	27	silty sand, silty clay	granite gneiss
M2	27	34	lateritic soil	granite gneiss
K1	0.4	9	silty gravel	quartzite
K2	1	8	silty sand	quartzite
K3	0.5	8	silty gravel	quartzite

*NF: Not found within the survey depth

obtained by dividing 30 m by the travel time from the surface to 30 m [18]. It is commonly used for site classification. Anbazhagan et al. [46] highlighted that V_s ^{30} is not the most reliable parameter for shallow bedrock sites and often represents stiffer site classes for sites with rock depths less than 25 m [3]. The average velocity up to bedrock depth would be a

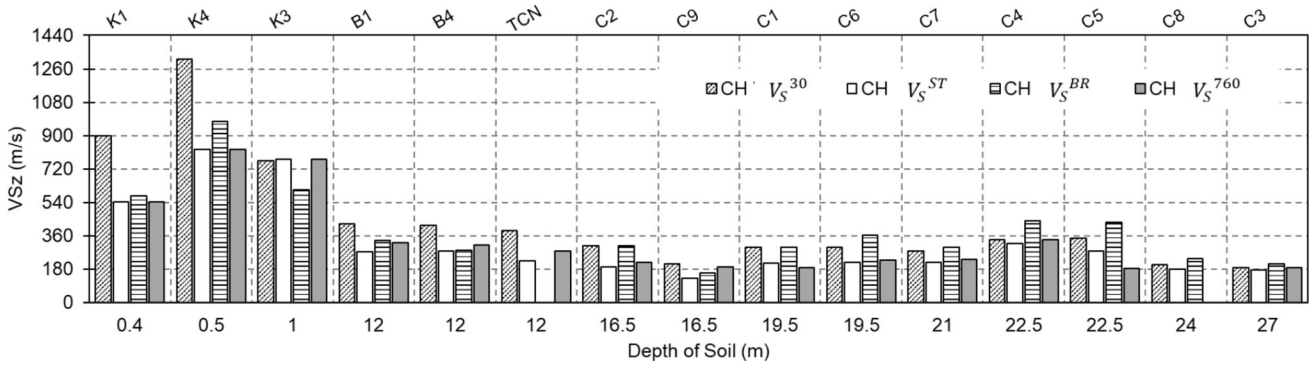

Fig. 17 V_S^z up to 30 m, Soil thickness, Bedrock depth and 760 m/s V_S depth for Crosshole test locations plotted against the soil depth obtained from the borelog V_S^{30}: Average Vs up to 30 m depth, V_S^{ST}: Average Vs up to Soil Thickness, V_S^{BR}: Average Vs up to Bedrock depth, V_S^{760}: Average Vs up to the stratum where V_S>760 m/s.

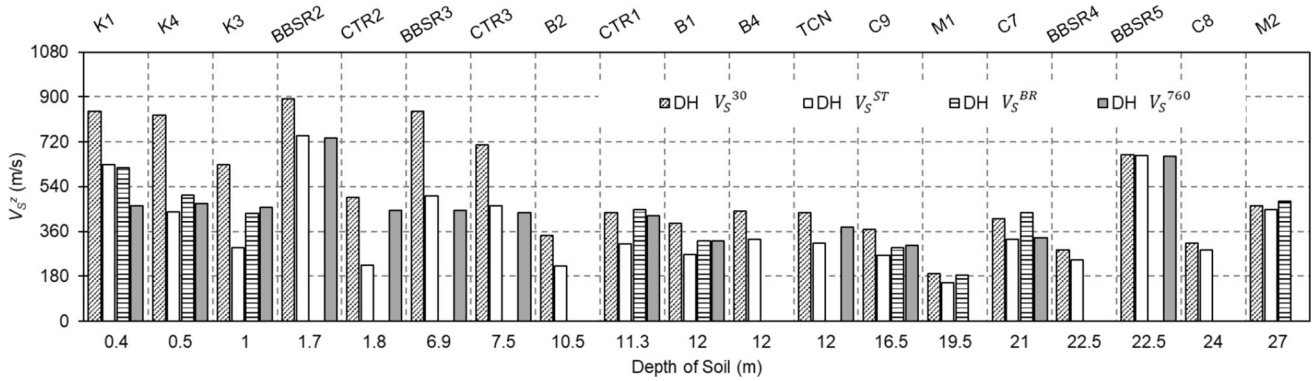

Fig. 18 $V_S{}^z$ up to 30 m, Soil thickness, Bedrock depth and 760 m/s V_S depth for downhole test locations plotted against the soil depth obtained from the borelog

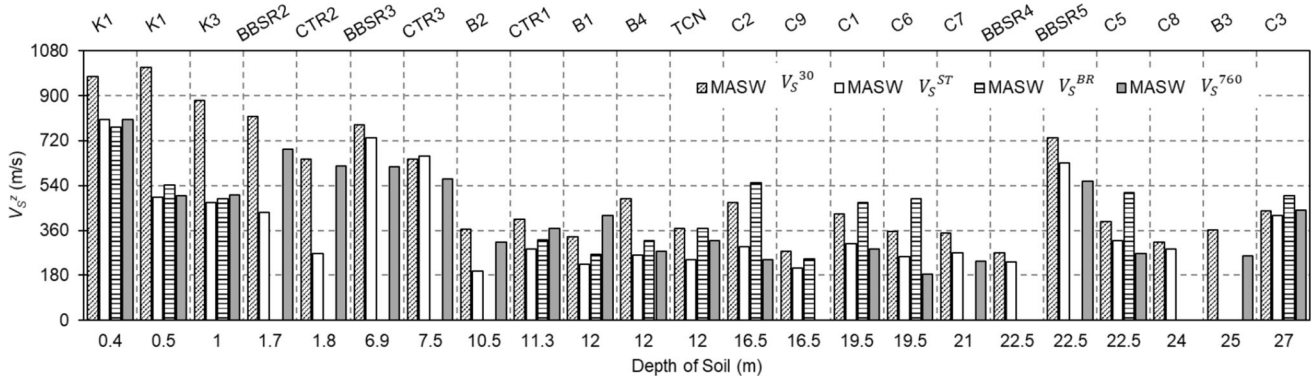

Fig. 19 $V_S{}^z$ up to 30 m, Soil thickness, bedrock depth and 760 m/s V_S depth for MASW test locations plotted against the soil depth obtained from the borelog

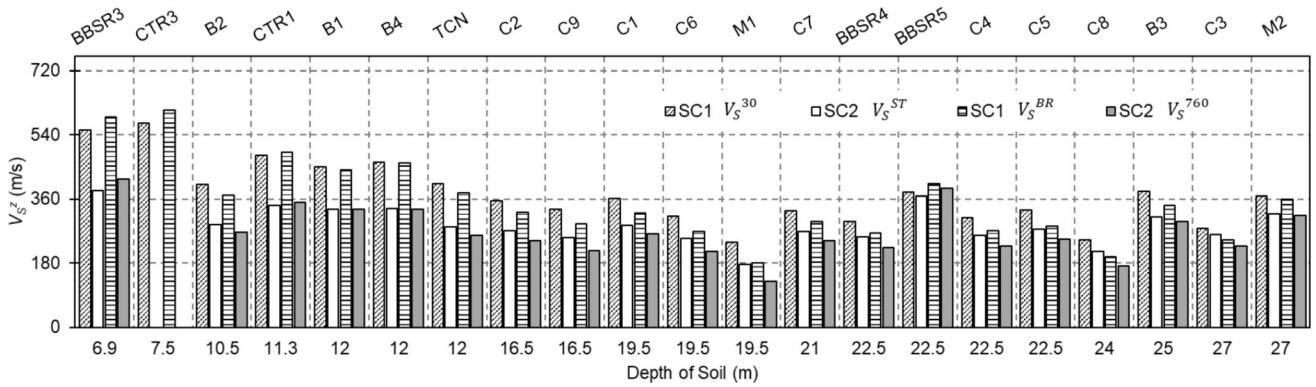

Fig. 20 $V_S{}^z$ up to 30 m, soil thickness and bedrock depth and 760 m/s V_S depth for V_S estimated from correlations plotted against the soil depth obtained from the borelog

better representative and has better correlations with site amplification. It has been found that weighted average shear stiffness is responsible for dynamic changes of the wave at the site. Many researchers use $V_s{}^{30}$, as it is related to seismic amplification. In this study, average velocities are estimated by adopting the following relation:

$$V_s^D = \frac{D = [\sum_{i=1}^{N} d_i]}{\sum_{i=1}^{N} \left(\frac{d_i}{v_i}\right)} \quad (1)$$

where d_i: the thickness of the i^{th} soil layer in metres; v_i: V_s for the i^{th} layer in *m/s* and n: no. of layers up to depth D or

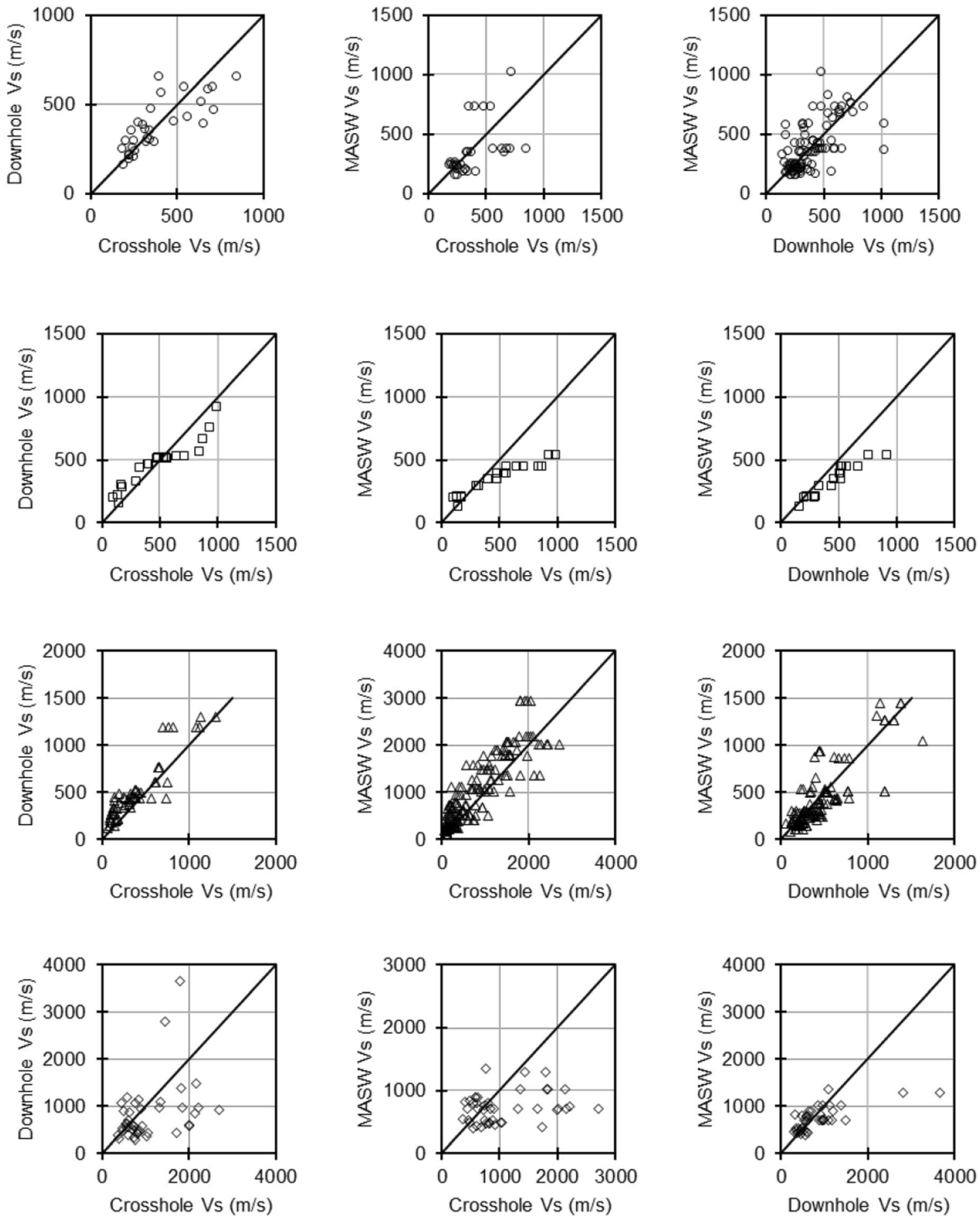

Fig. 21 **a** Comparison of V_S values from crosshole, downhole and MASW test for Residual deposits. **b** Comparison of V_S values from crosshole, downhole and MASW test for Coastal deposits. **c** Comparison of V_S values from crosshole, downhole and MASW test for Coastal alluvial deposits. **d** Comparison of V_S values from crosshole, downhole and MASW test for Quartzite rock formations. **e** Comparison of V_S values from MASW and downhole test for Lateritic deposits

the calculation layer. Here, D is considered as total thickness, i.e. from ground level to the base of the soil layer, or up to bedrock soil strata or 30 m, i.e. $V_s{}^{30}$.

Many design standards like Indian standard IS 1893 [35]) use depth averaged N values for site classification. The soil and rock sites are divided into three categories: Soft soils

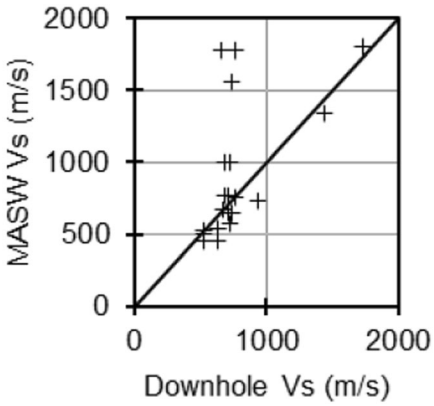

Fig. 21 continued

($N < 10$), medium or stiff soils ($10 \leq N < 30$) and Hard soils or rocks ($N \geq 30$). However, this method does not account for spatial variation of soil profiles, making it challenging to decide on the N value to be used for determining the soil profile type, which may include deep soil basins, sediment deposits, and the presence of weathered rocks among many others. NEHRP [20] provides site classification based on N values, including dense soil, soft rocks (Class I, N > 50), Stiff soil (Class II, 15 < N < 50) and soft soils (Class III, N < 15) along with respective $V_s{}^{30}$ values. Site classification based on BSSC [20] recommendations is given in Table 2. This study examines how different V_s measurement methods affect seismic site classes as presented in the following section.

7 Effect of method of V_s estimation on average V_s

7.1 *Estimation of* $V_S{}^{30}$ *for* V_S *profiles with depth < 30 m*

Often, the determination of $V_S{}^{30}$ using borehole methods is hindered by limiting the borehole depth well below 30 m, due to financial restrictions or rebound at a shallower depth. In such cases, $V_S{}^{30}$ cannot be calculated directly. However, a few extrapolation methods were proposed by Boore [16] to overcome this problem. One such method involves using average V_S up to the termination depth z ($V_S{}^z$) to estimate $V_S{}^{30}$. Based on the available dataset, linear correlations between $log\left(V_S{}^{30}\right)$ and $log(V_S{}^z)$ are obtained in the form of $log\left(V_S{}^{30}\right) = a + blog(V_S{}^z)$. The coefficients for different depths obtained after analysis of acquired data are presented in Table 3.

7.2 *Site classification based on* $V_S{}^{30}$ *and* N^{30}

Based on classification from the NEHRP method [20], $V_S{}^{30}$ and N^{30} values are calculated for the test locations. As discussed in Sect. 7.1, for the boreholes terminating before 30 m, extrapolation has been carried out as per Boore [16] for V_S and BSSC [20] for N-values. Most of the test sites were found to be in site class C or D, except for a few notable occurrences of E. Although $V_S{}^{30}$ helps assist in site classification and is useful for amplification estimation, it tells nothing about the variation in shallow subsurface dynamic properties. Any detail about shallow V_S profiles cannot be established with confidence and may be highly variable with depth which is observed only after studying the detailed profile. $V_S{}^{30}$ from different methods, N^{30} and corresponding site classes are presented in Table 4.

Sites for which N-values are not mentioned have near-surface bedrock, outcrop, or very stiff soil in shallow layers. Most of the deviations which occur are between class C and class D. The boundary between the two classes is $V_S{}^{30} = 360m/s$. Small difference in $V_S{}^{30}$ values close to the limiting values of site class is found to be more critical, e.g. for site B2, $V_S{}^{30}$ from the downhole test is 344 m/s, whereas from MASW survey, it is 364 m/s, which changes the site class from D to C. In some locations, the difference between $V_S{}^{30}$ values from different methods is large, although the class does not change, e.g. test location B4. The $V_S{}^{30}$ obtained from N-value correlations give the same site class as the other methods in most cases, with a few exceptions. Site class from N-values using N^{30} also results in the same site class as $V_S{}^{30}$ obtained from correlations, with a few exceptions. At location M1, a lower site class is estimated, class E using N^{30} which agrees with SC2, whereas class D is obtained from SC1 which is the same as DH. There are a few more locations as well where differences in site class using N^{30} and $V_S{}^{30}$ from SPT correlations is observed, which is between class C and D. Thus, in general, the site classification remains consistent, mostly between sites C and D, even though the $V_S{}^{30}$ values show large variations with changes in the method of survey.

Previously, Asten and Boore [7] suggested that neither the average shear velocity nor the 30 m depth limit is sufficient for adequate quantification of site response. More recently, limitations of using $V_S{}^{30}$ as a sole parameter for site classification and amplification estimation for site response studies were highlighted [12, 46]. A major disadvantage of $V_S{}^{30}$ is that it gives limited to no information about the proximity of bedrock to the ground surface. Anbazhagan et al. [3] showed that site class from $V_S{}^{30}$ without considering bedrock depth may lead to stiffer site classes for sites bedrock within top 25 m and softer site

classes for sites bedrock depth greater than 35 m. Anbazhagan et al. [46] recommended, based on the KiK-net data, that site effects caused by soil strata should be determined solely based on the soil parameters and that a separate velocity band should be established for shallow bedrock site classification. Using $V_S{}^{30}$ for shallow bedrock sites in site classification may result in overestimating the site class and underestimating site effects due to the high stiffness bedrock layer, as the velocity contrast between the soil layer and the bedrock will be much higher. Further, Bajaj and Anbazhagan [12] reviewed the studies with amplification factors derived from depths of $V_S \geq 760$ m/s and $V_S \geq 1500$ m/s and reported that inputting ground motion at layer with $V_S \geq 1500$ m/s would be more suitable for amplification estimation. $V_S \geq 760$ m/s and $V_S \geq 1500$ m/s are NEHRP site classification boundaries (Table 2) for average V_S values and are also considered engineering bedrock and weathered rock more often than hard rock.

Table 5 shows the soil thickness (which can also be considered as the depth of weathered rock, where SPT results in rebound and RQD is low or nil) and bedrock depth (considering RQD $\geq$ 50%, fair quality of rock) for the test locations. RQD from borelog is considered to

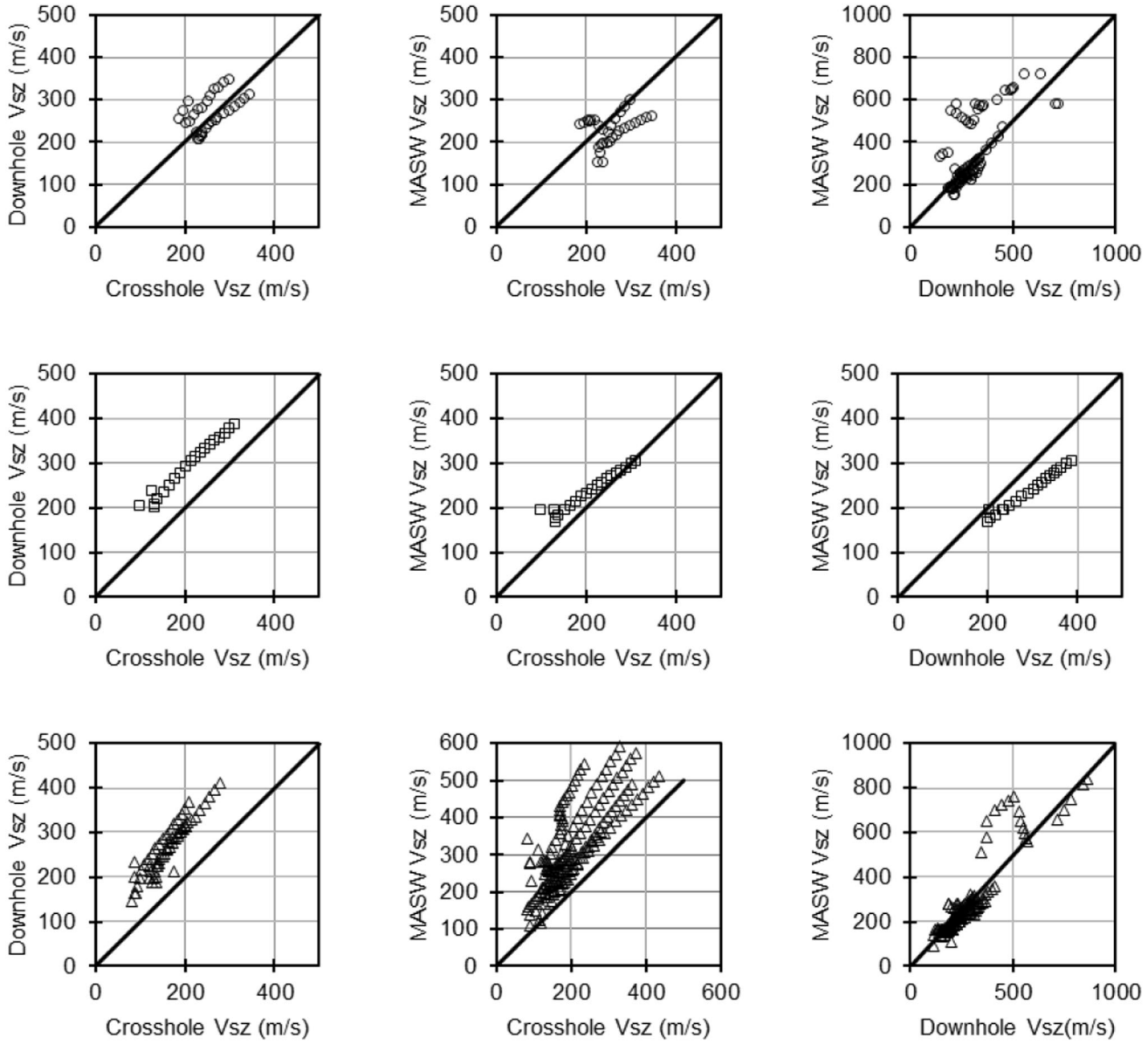

Fig. 22 **a** Comparison of $V_S{}^z$ values from crosshole, downhole and MASW test for Residual deposits. **b** Comparison of $V_S{}^z$ values from crosshole, downhole and MASW test for Coastal deposits. **c** Comparison of $V_S{}^z$ values from crosshole, downhole and MASW test for Coastal alluvial deposits. **d** Comparison of $V_S{}^z$ values from crosshole, downhole and MASW test for Quartzite rock formations. **e** Comparison of $V_S{}^z$ values from crosshole, downhole and MASW test for Lateritic deposits

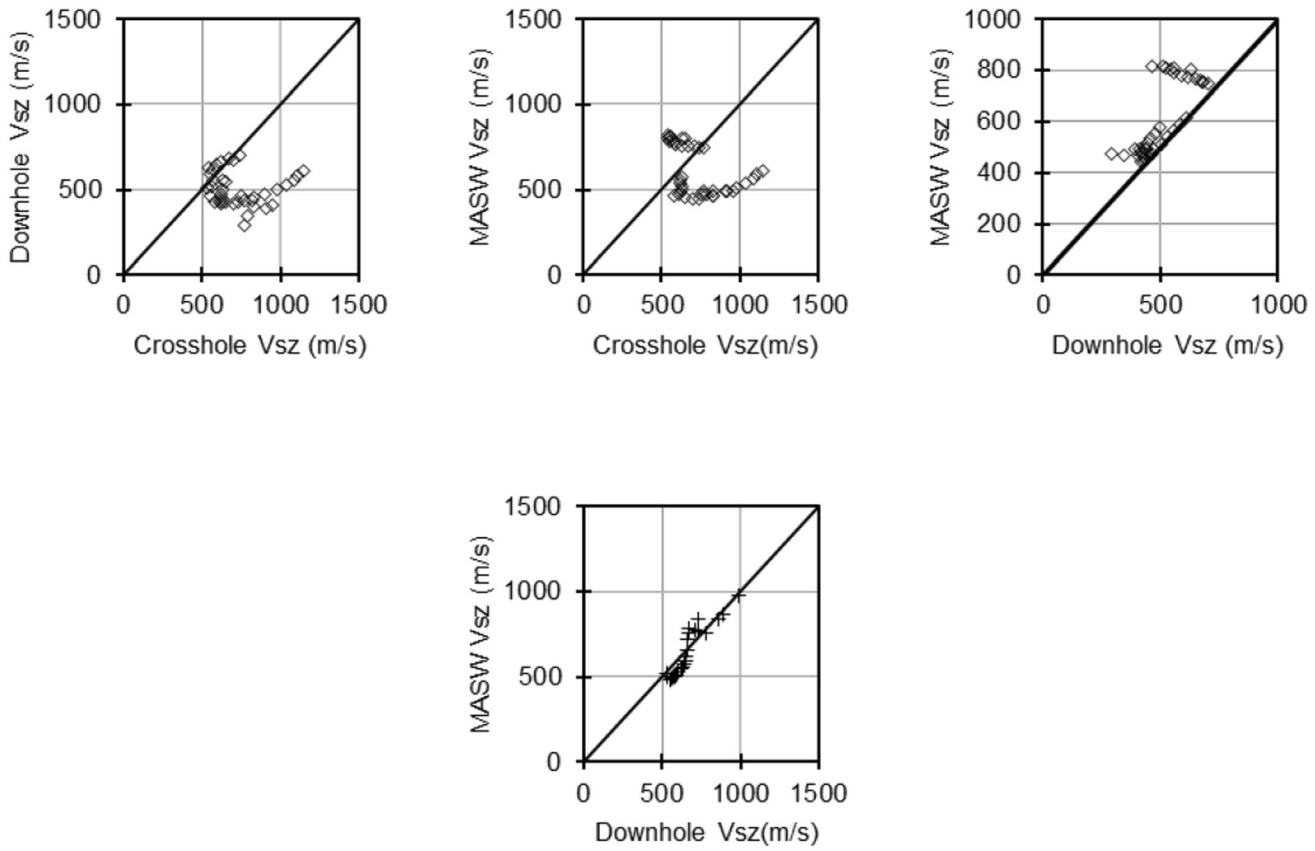

Fig. 22 continued

interpret weathered rock and hard rock strata, instead of using V_S value of 760 m/s and 1500 m/s from V_S profiles because of two reasons:

(1) The V_S profiles for many test locations do not extend up to the depth where $V_S \geq 1500$ m/s.
(2) Different methods result in different V_S profiles; hence, one bedrock depth cannot be established considering only V_S profiles.

Based on Tables 4 and 5, and Figs. 17, 18, 19 and 20, it can be observed that locations with shallower sediment depth or bedrock depth can have lower site class than the sites with higher sediment or bedrock depth. Even the sites with the same sediment depth can have a huge difference in $V_S{}^{30}$ value in the same or different geology and hence the difference in site class as well. Although a general perception is that shallow sites should have a higher site class than those having deeper bedrock depths. Peninsular India is a shallow bedrock region, and in this region, often, the bedrock occurs within the top 30 m, hence $V_S{}^{30}$ may not be a representative parameter for site classification and response analysis. More emphasis must be given to the sediment properties, bedrock depth, and rock characteristics. Figures 17, 18, 19 and 20 present $V_S{}^{z}$ values up to different depths compared with each other in the site classification spectrum. Average V_S up to 30 m is $V_S{}^{30}$, average V_s up to soil thickness (ST) is $V_S{}^{ST}$, average V_s up to bedrock depth (BR) $V_S{}^{BR}$ and average V_S up to the depth where V_S exceeds 760 m/s is $V_S{}^{760}$. These plots show how different average V_S values in the same site vary with V_s measurement methods. $V_S{}^{30}$ is higher than $V_S{}^{ST}$ generally, as the soil thickness is mostly less than 25 m. It is discussed in previous sections how sites with bedrock depth less than 25 m are susceptible to overestimation of site class. Since Peninsular India is a shallow bedrock region, with bedrock shallower than 30 m, $V_S{}^{30}$ will be generally greater than $V_S{}^{BR}$.

At some locations, even the site class changes if the $V_S{}^{z}$ values for site classification are kept the same as NEHRP scheme. Moreover, change in survey method also affects $V_S{}^{ST}$, $V_S{}^{BR}$ and $V_S{}^{760}$. For example, at test location C8, both D and E site classes are obtained; the same is observed for M1. Further, for $V_S{}^{BR}$, similar observations are made for C9 (class E and D), CTR1, C2, C1, C7 and C3 (class D and C). Thus, change in the survey method may lead to entirely different interpretations of site behaviour, in determining site class for response studies. This observation accompanies above highlights that for one method

itself, there can be many average V_s interpretations based on the target depth of input ground motion.

This study also highlights the limitations of $V_S{}^{30}$ as the sole parameter for site classification and response studies in shallow bedrock, especially if the sediment depth is less than 25 m with low average V_S. Average properties up to sediment thickness or average properties up to the bedrock depth shall better indicate site classification in shallow bedrock regions. Although seismic classification using top 30 m depth is very common in shallow bedrock sites, $V_S{}^{30}$ often overestimates site class due to the presence of rock in shallow depths. Impedance contrast can cause more amplification than what is indicated from input motion at 30 m depth. A site-specific study may be more appropriate for dealing with these sites.

8 Conclusions

In this study, site exploration involving SPT and V_s measurements from crosshole, downhole and MASW surveys was obtained in shallow bedrock sites in the different geological formations, in peninsular India. Two correlations previously established for this region were also used to estimate V_s from N-values. V_s profiles from different methods were comparable, except at a few sites where the difference is significant due to inconsistency of impedance contrast or bedrock layers. To quantify the variability in V_s profiles, the coefficient of variation (COV) for all the depths was calculated and was observed to be mostly confined within 30%, with a few occurrences of reaching as high as 50–60% at coastal locations.

At residual, coastal and coastal alluvial locations, CH and DH tests result in similar V_s values up to layer with V_s of 500 m/s. For coastal alluvial test locations, the MASW profiles result in higher values than other V_s profiles, mainly due to shallower bedrock depth estimation. In case of quartzite locations, CH profiles are way off when compared to DH and MASW profiles. Another observation from 1:1 comparison of V_s profiles is that if one method results in a few higher V_S values than the second, still the second method can result in a higher $V_S{}^{Z}$ profile. Subsurface profiling is also affected by lateral spread of soil and rock layers. This study found that if subsurface layers are spatially homogeneous and V_s increases with depth, then all methods lead to almost similar results. When subsurface layers are non-homogeneous and consist of alternate layers of varying stiffness, V_s profiles are prone to deviations from true profile with minimum deviation in CH followed by DH, SPT correlations and MASW.

Using the V_s profiles and borelogs, $V_s{}^{30}$ was calculated for site class estimation. Site class was not much affected by the variability in V_s profiles due to different methods of measurement. This is possible due to a wide range of $V_s{}^{30}$ for site classes above D. At a few locations, even with less scatter in V_s values, the $V_s{}^{30}$ values from different methods give different site classes because of proximity to the limiting $V_s{}^{30}$ value. The SPT N-values were used for site classification using N^{30} and $V_s{}^{30}$ from correlations available for the region. Except in a few cases, using the two methods, the site class obtained was the same as the class from $V_s{}^{30}$, mostly varying between class C and class D. This observation highlights that the SPT data, when used differently, can result in different site classes at the same location. Further, the average V_s up to the bedrock depth, soil thickness depth and layer with $V_s \geq 760$ m/s were also calculated. These average values, considering the same $V_s{}^{z}$ boundaries as NEHRP classification, show different classes for the same test location when compared to $V_s{}^{30}$. Since $V_s{}^{30}$ also includes V_S from rock layers in shallow bedrock regions, its applications for such regions are questionable if the sediment deposit is prone to site effects.

Appendix

See (Figs. 21 and 22).

The figures in this section are extensions of Fig. 15 and Fig. 16, showing a comparison of V_S values obtained from the three survey methods: crosshole, downhole and MASW.

It is worth noting that the scatter present in the V_S data points in Fig. 21 reduces significantly in $V_S{}^{Z}$ in Fig. 22. This is because averaging of V_S over depth prevents any sharp changes in $V_S{}^{Z}$. However, $V_S{}^{Z}$ helps in better identification of comparison trends between two methods at any location or geology. Figure 22 also shows the relation between $V_S{}^{Z}$ obtained from the two methods can be expressed in a simple relation, much better than V_S.

Another observation from both the figures is that if one method results in a few higher V_S values than the second, still the second method can result in a higher $V_S{}^{Z}$. For example, in Fig. 21b, crosshole gives a few V_S values higher than that of downhole test. However, when we see Fig. 22b, downhole has a higher $V_S{}^{Z}$ for all the data points. Similar observations can be noted in for other locations in Fig. 21b, Fig. 22b, Fig. 21c, Fig. 22c, Fig. 21d and Fig. 22d as well.

Acknowledgements The authors thank Mr. Ravinesh Kumar and Mr. Siriwanth Kumar, Research Assistants; Mr. Kamalhassan, Project Intern; and Ms. Divyasree Varadaraj, Project Staff, Department of Civil Engineering, Indian Institute of Science, for their valuable contribution during field testing and processing of field data.

Author contributions Ayush Kumar contributed to conceptualization, methodology, formal analysis and investigation, writing—original draft preparation, and writing—review and editing. Anbazhagan Panjamani contributed to conceptualization, writing—review and editing, funding acquisition, resources, and supervision.

Funding This work was supported by the Dam Safety (Rehabilitation) Directorate, Central Water Commission, Govt. of India for the project entitled "Capacity Buildings in Dam Safety" under Dam Rehabilitation and Improvement Project"; SERB, DST, Govt. of India for the project "Development of correction factors for standard penetration test N values in India through energy measurement and field experiments—Step towards a reliable Liquefaction Potential Assessment" under Grant SERB/F/198/2017–18 dated 11/05/2017; and M/s Secon Pvt. Ltd. for the project "Effect of shear wave velocity calibration on Amplification of shallow and deep soil sites" under grant SECON/IISc/MoES/WO/07–18/0079.

Data availability No datasets were generated or analysed during the current study.

Declarations

Conflict of interest The authors declare no competing interests.

References

1. Anbazhagan P, Bajaj K, Reddy GR, Phanikanth VS, Yadav DN (2016) Quantitative assessment of shear wave velocity correlations in the shallow bedrock sites. Indian Geotechn J Springer India 46(4):381–397
2. Anbazhagan P, Kumar A, Ingale SG, Jha SK, Lenin KR (2021) Shear modulus from SPT N-values with different energy values. Soil Dyn Earthq Eng 150:106925
3. Anbazhagan P, Sheikh MN, Parihar A (2013) Influence of rock depth on seismic site classification for shallow bedrock regions. Nat Hazard Rev 14(2):108–121
4. Anbazhagan P, Sitharam TG (2009) Spatial variability of the depth of weathered and engineering bedrock using multichannel analysis of surface wave method. Pure Appl Geophys 166(3):409–428
5. Anbazhagan P, Uday A, Moustafa SSR, Al-Arifi NSN (2016) Correlation of densities with shear wave velocities and SPT N values. J Geophys Eng 13(3):320–341
6. Anderson N, Thitimakorn T, Ismail A, Hoffman D (2007) A comparison of four geophysical methods for determining the shear wave velocity of soils. Environ Eng Geosci 13(1):11–23
7. Asten M, Boore D (2005) Comparison of shear-velocity profiles of unconsolidated sediments near the coyote borehole (CCOC) measured with fourteen invasive and non-invasive methods. J Environ Eng Geophys 10(2):85
8. Asten MW, Stephenson WR, Davenport PN (2005) Shear-wave velocity profile for holocene sediments measured from microtremor array studies, SCPT, and seismic refraction. J Environ Eng Geophys 10(3):235–242
9. D4428–14 (2014) *Standard Test Methods for Crosshole Seismic Testing (withdrawn). ASTM International*.
10. Badreldin H, El-Ata AA, El-Hadidy M, Cornou C, Lala AM (2023) Active and passive seismic methods for site characterization in Nuweiba, Gulf of Aqaba, Egypt. Soil Dyn Earthq Eng 172:108002
11. Bajaj K, Anbazhagan P (2021) Identification of shear modulus reduction and damping curve for deep and shallow sites: kik-net data. J Earthq Eng Taylor Franc 25(13):2668–2696
12. Bajaj K, Anbazhagan P (2022) Site amplification factors and acceleration response spectra for shallow bedrock sites-application to Southern India. J Earthq Eng Taylor Franc 26(4):2103–2123
13. Bajaj K, Anbazhagan P (2023) Effective input velocity and depth for deep and shallow sites for site response analysis. Geomech Geoeng Taylor Franc 18(3):193–207
14. Bang ES, Cho SJ, Kim DS (2014) Mean refracted ray path method for reliable downhole seismic data interpretations. Soil Dyn Earthq Eng 65:214–223
15. Boaga J, Vignoli G, Cassiani G (2011) Shear wave profiles from surface wave inversion: the impact of uncertainty on seismic site response analysis. J Geophys Eng 8(2):162–174
16. Boore DM (2004) Estimating Vs(30) (or NEHRP Site Classes) from shallow velocity models (Depths < 30 m). Bull Seismol Soc Am 94(2):591–597
17. Boore DM, Asten MW (2008) Comparisons of shear-wave slowness in the Santa Clara Valley, California using blind interpretations of data from invasive and noninvasive methods. Bull Seismol Soc Am 98(4):1983–2003
18. Borcherdt RD (1994) Estimates of site-dependent response spectra for design (Methodology and Justification). Earthq Spectra 10(4):617–653
19. Brown LT, Boore DM, Stokoe KH (2002) Comparison of shear-wave slowness profiles at 10 strong-motion sites from noninvasive SASW measurements and measurements made in boreholes. Bull Seismol Soc Am 92(8):3116–3133
20. BSSC (2003) *NEHRP Recommended Provisions for Seismic Regulations for New Buildings and Other Structures (FEMA 450). Part 1*, Building Seismic Safety Council.
21. Butler DK, Curro JR (1981) Crosshole seismic testing—procedures and pitfalls. Geophysics 46(1):23–29
22. Castellaro S, Mulargia F, Rossi PL (2008) Vs30: proxy for seismic amplification? Seismol Res Lett 79(4):540–543
23. Chandran D, Anbazhagan P (2020) 2D nonlinear site response analysis of typical stiff and soft soil sites at shallow bedrock region with low to medium seismicity. J Appl Geophys 179:104087
24. Cornou, C., Ohrnberger, M., Boore, D. M., Kudo, K., and Bard, P.-Y (2006) "Derivation of structural models from ambient vibration array recordings: results from an international blind test." *Third International Symposium on the Effects of Surface Geology on Seismic Motion*, (September), 1127–1219.
25. Cox, B. R., Wood, C. M., and Teague, D. P. (2014). "Synthesis of the UTexas1 Surface Wave Dataset Blind-Analysis Study: Inter-Analyst Dispersion and Shear Wave Velocity Uncertainty." 850–859.
26. Crice D (2011) Near-surface, downhole shear wave surveys- a primer. Lead Edge 30(2):164–171
27. D7400–19 (2019) "Standard Test Methods for Downhole Seismic Testing." *ASTM International*, 1–11.
28. Darko AB, Molnar S, Sadrekarimi A (2020) Blind comparison of non-invasive shear wave velocity profiling with invasive methods at bridge sites in Windsor, Ontario. Soil Dyn Earthq Eng 129(2019):105906
29. Deere, D. U., and Deere, D. W (1988) "The rock quality designation (RQD) index in practice." *ASTM Special Technical Publication*.
30. Dettmer J, Molnar S, Steininger G, Dosso SE, Cassidy JF (2012) Trans-dimensional inversion of microtremor array dispersion data with hierarchical autoregressive error models. Geophys J Int 188(2):719–734

31. Fernandez JA, Rix GJ, Gowdy S (2008) Inversion algorithm to evaluate velocity profiles from downhole seismic tests. American Society of Civil Engineers, Reston, VA, Geotechnical Earthquake Engineering and Soil Dynamics IV, pp 1–10
32. Foti S, Parolai S, Bergamo P, Giulio GD, Maraschini M, Milana G, Picozzi M, Puglia R (2011) Surface wave surveys for seismic site characterization of accelerometric stations in ITACA. Bull Earthq Eng 9(6):1797–1820
33. Garofalo F, Foti S, Hollender F, Bard PY, Cornou C, Cox BR, Dechamp A, Ohrnberger M, Perron V, Sicilia D, Teague D, Vergniault C (2016) InterPACIFIC project: comparison of invasive and non-invasive methods for seismic site characterization. Part II: inter-comparison between surface-wave and borehole methods. Soil Dyn Earthq Eng 82:241–254
34. Garofalo F, Foti S, Hollender F, Bard PY, Cornou C, Cox BR, Ohrnberger M, Sicilia D, Asten M, Di Giulio G, Forbriger T, Guillier B, Hayashi K, Martin A, Matsushima S, Mercerat D, Poggi V, Yamanaka H (2016) InterPACIFIC project: comparison of invasive and non-invasive methods for seismic site characterization. Part I: intra-comparison of surface wave methods. Soil Dyn Earthq Eng 82:222–240
35. IS 1893 (2016) *Criteria for Earthquake Resistant Design of Structures - Part I: General Provisions and Buildings*. Bureau of Indian Standards.
36. Kim DS, Bang ES, Kim WC (2004) Evaluation of various downhole data reduction methods for obtaining reliable VS profiles. Geotech Test J 27(6):585–597
37. Kim JH, Park CB (2002) Processing of downhole S-wave seismic survey data by considering direction of polarization. J Korean Geophys Soc 5(4):321–328
38. Kim, D. S., Park, H. J., and Bang, E. S (2013) "Round Robin test for comparative study of in-situ seismic tests." *Geotechnical and Geophysical Site Characterization 4 - Proceedings of the 4th International Conference on Site Characterization 4, ISC-4*, 2, 1427–1434.
39. Kumar A, Anbazhagan P (2023) Integration of downhole data reduction techniques for determination of Vs profiles. Geo-Congress 2023:152–161
40. Kumar KS, Kishore PP, Srinivas GS, Prasad PP, Seshunarayana T (2018) Application of crosshole seismic technique and MASW at heavy engineering site, near Mahabalipuram, Tamilnadu. J Indian Geophys Un 22(3):279–285
41. Lin, Y (2008) "Variability in Vs Profiles and Consistency between Seismic Profiling Methods: A Case Study in Imperial Valley, California." *Proceeding of the 3rd International Conference on Site Characterization (ISC'3).*, Taipei, Taiwan.
42. Liu, S., Ebel, J. E., Urzua, A., and Murphy, V (2018) "Shear-wave velocity analysis by surface-wave methods in the Boston area." *11th National Conference on Earthquake Engineering 2018, NCEE 2018: Integrating Science, Engineering, and Policy*, 12, 7703–7713.
43. Maheswari RU, Boominathan A, Dodagoudar GR (2010) Use of surface waves in statistical correlations of shear wave velocity and penetration resistance of Chennai soils. Geotech Geol Eng 28(2):119–137
44. Michaels P (2001) Use of principal component analysis to determine down-hole tool orientation and enhance SH-Waves. J Environ Eng Geophys Environ Eng Geophys Soc 6(4):175–183
45. Molnar S, Ventura CE, Boroschek R, Archila M (2015) Site characterization at Chilean strong-motion stations: comparison of downhole and microtremor shear-wave velocity methods. Soil Dyn Earthq Eng 79:22–35
46. Panjamani A, Kumar Katukuri A, Gr R, Moustafa SS, Al-Arifi NS (2018) Seismic site classification and amplification of shallow bedrock sites. Plos One 13(12):e0208226
47. Park, C. B (2005) *MASW – Horizontal Resolution in 2D Shear-Velocity (Vs) Mapping KGS Open-File Report 2005–4*.
48. Park, C. B., Miller, R. D., and Miura, H (2002) "Optimum field parameters of an MASW survey." *Proceedings of the Society of Exploration Geophysicists (SEG) Japan Tokyo*, 22, 23.
49. Park CB, Miller RD, Xia J (1999) Multichannel analysis of surface waves. Geophysics 64(3):800–808
50. Rahman MZ, Siddiqua S, Kamal ASMM (2016) Shear wave velocity estimation of the near-surface materials of Chittagong City, Bangladesh for seismic site characterization. J Appl Geophys 134:210–225
51. Roblee, C., Stokoe, K., Fuhriman, M., and Nelson, P (1994) "Crosshole SH-Wave Measurements in Rock and Soil." *Dynamic Geotechnical Testing II*, ASTM International100 Barr Harbor Drive, PO Box C700, West Conshohocken, PA 19428-2959, 58–72
52. Stolte AC, Cox BR (2020) Towards consideration of epistemic uncertainty in shear-wave velocity measurements obtained via seismic cone penetration testing (SCPT). Can Geotech J 57(1):48–60
53. Wightman, W., et al, Jalinoos, F., Sirles, P., and & Hanna, K (2004) *Application of geophysical methods to highway related problems (No. FHWA-IF-04–021)*.
54. Wu W, Liu J, Guo L, Deng Z (2020) Methodology and assessment of proxy-based Vs30 estimation in Sichuan Province, China. Int J Disaster Risk Sci 11(1):133–144
55. Xia J, Miller RD, Park CB (1999) Estimation of near-surface shear-wave velocity by inversion of Rayleigh waves. Geophys Soc Explor Geophys 64(3):691–700
56. Yilmaz, O., Eser, M., Sandikkaya, A., Akkar, S., Bakir, S., and Yilmaz, T (2008) "Comparison of shear-wave velocity-depth profiles from downhole and surface seismic experiments." *14th World Conference on Earthquake Engineering, Pekin, China*, (2008).
57. Zhou J, Li L, Li XJ, Yu YX, Tian QJ (2023) Lateral variations of shear wave velocity (VS) profile and VS30 over gentle terrain. Soil Dyn Earthq Eng 175:108265